



# Hydrothermal Co-Liquefaction of Food Waste and Lignin

A Major Qualifying Project

Submitted to the faculty of

WORCESTER POLYTECHNIC INSTITUTE

In partial fulfillment of the requirements for the

Degree of Bachelor of Science

In Chemical Engineering

By: Skyler Kauffman

To: Michael T Timko (Advisor),

Alex R Maag (Advisor)

April, 2024

*This report represents work of one or more WPI undergraduate students submitted to the faculty as evidence of completion of a degree requirement. WPI routinely publishes these reports on the web without editorial or peer review. For more information about the projects program at WPI, see <http://www.wpi.edu/Academics/Projects>.*

# Table of Contents

Table of Figures .....	4
1.0 Abstract.....	6
2.0 Background.....	7
2.1 Waste to Energy .....	7
2.2 Hydrothermal Liquefaction.....	11
2.3 Co-Fed HTL.....	13
2.4 Food Waste and Lignin .....	15
2.5 Cosolvent Enhanced Lignocellulosic Fractionation .....	17
2.6 Motivation.....	18
3.0 Methods.....	20
3.1 Hydrothermal Liquefaction: Setup .....	20
3.2 Hydrothermal Liquefaction: Separations .....	23
3.3 Elemental Analysis.....	29
3.4 Total Organic Carbon Analysis .....	32
3.5 Karl Fischer Titration.....	35
3.6 Gas Chromatography with Mass Spectrometry .....	37
3.7 Safety Considerations .....	38
4.0 Results and Discussion .....	40
4.1 Mass Yields.....	40
4.2 Moisture Content .....	41
4.3 Carbon Content.....	43
4.4 Carbon Balances .....	46
4.5 Gas Chromatography with Mass Spectrometry .....	51
5.0 Conclusion .....	54
6.0 Recommendations.....	56
7.0 Future Work .....	57
8.0 Acknowledgements.....	58
References.....	59
Appendix.....	62
Appendix A: Selected images of feed and reactor setup.....	62

Appendix B: Sample instrument reports and tracking sheets ..... 69  
Appendix C: Tables of Data..... 74

# Table of Figures

Figure 1: Global greenhouse gas emissions by sector [1].....	9
Figure 2: EPA review of the environmental footprint of food loss and waste [6] .....	10
Figure 3: Symbolic representation of HTL process .....	11
Figure 4: Schematic representation of typical HTL reaction pathways. The feed decomposes into small organics and polymerizes into the solid phase. As the reaction progresses, small organics repolymerize into biocrude and solid and further decompose into gas [10].....	13
Figure 5: Illustration of synergistic and antagonistic effects observed for mixed feed HTL of biomass and food waste [11]......	15
Figure 6: Schematic representation of CELF process for lignin isolation [18] .....	18
Figure 7: Flow diagram for overall waste-to-energy process for HTL of food waste and lignin .	19
Figure 8: Feed and water are added to the reactor in preparation for HTL .....	21
Figure 9: The reactor is purged with nitrogen gas .....	22
Figure 10: The HTL reaction is completed, generating oil, solid, aqueous, and gas phase products .....	23
Figure 11: The reactor is cooled in an ice bath, then the reactor head is removed after depressurization .....	25
Figure 12: The solid and aqueous products of the HTL reactions are separated via vacuum filtration.....	26
Figure 13: The solid filter cake is washed with acetone, removing the biocrude product.....	28
Figure 14: Rotary evaporation is used to isolate the oil product from acetone .....	29
Figure 15: Average mass yields observed for each product phase as a function of feed fraction PKFW. Ratios range from 0% PKFW feed on the left to 100% PKFW feed on the right. Error is reported as +/- one standard deviation for at least two trials for each ratio.....	40
Figure 16: Average oil moisture content as a function of feed fraction PKFW. Oils with a lower PKFW feed fraction had moisture contents up to 66%.....	42
Figure 17: Moisture-corrected average elemental compositions for oils produced at various feed ratios. Data for oils produced with 0% PKFW feed are omitted due to high moisture content....	43
Figure 18: Moisture-corrected average elemental compositions for the solid product phase of mixed feed HTL reactions with various feed ratios. ....	44

Figure 19: Heuristically predicted higher heating value for oils produced using various feed ratios. Data for oils produced with 0% PKFW feed are omitted due to high moisture content....	46
Figure 20: Average carbon yields for each product phase of HTL reactions with various feed ratios of PKFW and lignin. ....	47
Figure 21: Carbon yield as a function of feed ratio for oil .....	48
Figure 22: Carbon yield as a function of feed fraction for solid products .....	48
Figure 23: Carbon yield as a function of feed fraction for aqueous phase products .....	49
Figure 24: Carbon yield as a function of feed fraction for gas phase products .....	49
Figure 25: Dissolved carbon in aqueous phase as a function of feed fraction PKFW .....	50
Figure 26: GCMS chromatograms for oils produced using various feed ratios of PKFW and lignin .....	51
Figure 27: Significant molecular components of oil produced using a 50% PKFW feed ratio, as determined by GCMS. ....	52

# 1.0 Abstract

The world produces millions of tons of food waste and lignin annually, the disposal of which has massive environmental impacts. An estimated 8% of cumulative global greenhouse gas emissions have been caused by food waste alone. Waste-fed biocrude, which may be upgraded into a sustainable and energy-dense biofuel, may replace fossil fuels and offset environmental damage caused by organic waste disposal. Hydrothermal co-liquefaction of mixed waste feeds is a promising technology capable of increasing biocrude yields compared to traditional single-feed hydrothermal liquefaction (HTL). Mixing HTL feeds often enables new chemical pathways, leading to synergistic or antagonistic effects on product yield. This study examines the effect of mixing food waste and lignin at various ratios for mixed-feed HTL reactions. Reactions were carried out at standard HTL conditions of 300 °C and 60 minutes. Elemental analysis, total organic content analysis, Karl Fisher titration, and gas chromatography with mass spectrometry (GCMS) were used to characterize the reaction products. Feed ratio had a negligible impact on product distribution outside of mixing effects, suggesting a lack of significant synergistic or antagonistic interactions between feeds. However, several compounds were identified by GCMS solely in mixed feed oils, notably fatty acid methyl esters. Novel chemistry was observed between food waste and lignin, but it was not significant enough to impact product yields or oil quality.

## 2.0 Background

### 2.1 Waste to Energy

Much of the environmental crisis facing the world today is caused directly or indirectly by unsustainable energy production and waste disposal practices. A total of 33.7% of global carbon emissions in 2016 were caused by energy use in buildings and transportation. Another 3.2% were caused by landfills and wastewater processing [1]. While high levels of carbon dioxide in the atmosphere is only one among many factors causing the global environmental crisis, it is one of the most well-understood and easy to quantify. Since the beginning of the industrial revolution, carbon dioxide concentration in the atmosphere has increased from 280 ppm in the mid 1700s to 414.7 ppm in 2021 [2]. This is the highest concentration in at least three million years. Carbon dioxide is known to behave as a greenhouse gas, trapping heat on the Earth's surface instead of allowing it to escape. This has led to increasing global average temperatures. Temperatures have already increased 0.86 °C compared to the 19<sup>th</sup> century average. The previous nine years (2014-2022) are the warmest years ever recorded. This increased temperature has a multitude of negative effects including destruction of habitats, excessive rainfall, reduced snowfall, and rising sea levels [3]. About two thirds of this heating is estimated to be due to human-caused carbon dioxide emission [2].

The vast majority of human-caused carbon dioxide emissions have been due to the burning of fossil fuels. Since the start of the industrial revolution, fossil fuels have served as a cheap and abundant source of energy. Their energy density and ease of transport continue to make them appealing despite their harmful effects. Renewable energy sources such as wind, solar, geothermal, and hydroelectric have become increasingly popular as an alternative. Nuclear

energy has also been widely used as a carbon-free source of energy for decades. However, these solutions typically require large, expensive, and stationary installations. While typical renewables can replace fossil fuels relatively easily for electricity generation, they are less useful for transportation. Sustainably produced energy must be stored in batteries for use in transportation. These batteries are slow to charge, massively heavy, and environmentally destructive to produce. Aviation in particular poses a challenge for adoption of renewable energy: the energy density of modern batteries is not nearly high enough for use in an aircraft. The energy density of jet fuel is 43 MJ/kg, while the energy density of a battery used in a typical electric vehicle is only 0.72 MJ/kg [4]. Because of this, development of sustainable aviation fuels to replace petroleum-based jet fuels is highly appealing.



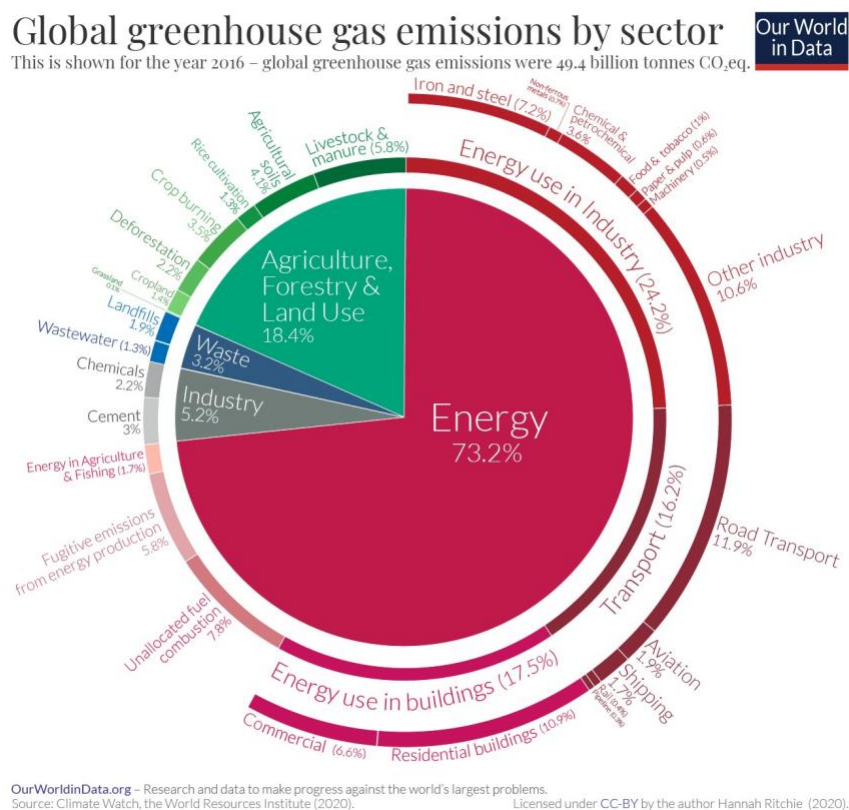














Figure 1: Global greenhouse gas emissions by sector [1]

While the bulk of carbon emissions are caused by the burning of fossil fuels, food production and disposal also play a large part. Agriculture, forestry, and land use contribute 18.4% to global carbon emissions. The US produces roughly 15 million dry tons of food waste per year, most of which ends up in landfills and contributes to greenhouse gas emission [5]. Food production is a resource-intensive process, requiring massive land, water, energy, pesticide, and fertilizer usage. Pesticides and fertilizer make their way into farm runoff, causing toxic pollution and algal blooms. Once produced, food must be quickly transported and stored, contributing further to energy usage and greenhouse gas emissions. In fact, approximately 8% of historical human-caused greenhouse gas emissions have been the result of food loss and waste [6]. Figure 2 helps visualize the various environmental effects of food production.

Environmental Impact	Environmental Footprint				Source Scope of FLW
	Total (Standard Units)	Per Person	Percentage of U.S. Cradle-to-Consumer Food System Footprint	Percentage of U.S. Footprint	
 Land Use	560,000 km <sup>2</sup> • (140 million acres)	1,800 m <sup>2</sup> <sup>¶</sup> (19,000 sq ft)	16% of agricultural land •	–	Read et al. (2020) 
 Water Use <sup>a</sup>	22 trillion L • (5.9 trillion gallons)	71,000 L <sup>¶</sup> (19,000 gallons)	17% of freshwater used •	5%	Read et al. (2020) 
 Pesticide Application	350 million kg <sup>b</sup> (780 million pounds)	1 kg • (2.5 pounds)	–	–	Conrad et al. (2018) 
 Fertilizer Application	6,350 million kg • (14 billion pounds)	20.2 kg <sup>•, b</sup> (44.5 pounds)	42% of total fertilizers used	–	Toth and Dou (2016) 
 Energy Use	2,400 million GJ (664 billion kWh)	7.7 GJ • (2,140 kWh)	20% of energy used	2%	Pagani et al. (2020); Vittuari et al. (2020) 
 GHG Emissions	170 million MTCO <sub>2</sub> e •	540 kg CO <sub>2</sub> e <sup>¶</sup>	16% of GHG emissions •	2%	Read et al. (2020) 

• = calculated

¶ = personal communication with author

<sup>a</sup> Blue water use.

<sup>b</sup> Accounts for only consumer FLW

*Figure 2: EPA review of the environmental footprint of food loss and waste [6]*

Conversion of waste to energy-dense fuels has the potential to help alleviate both problems; biofuel is an energy-dense fuel that helps reduce the harmful effects of food waste. Biofuel captures energy in food that would otherwise go unused, and its production from waste decreases greenhouse gas emission from landfills. While there are several technologies that may be used to convert waste into fuels, including anaerobic digestion [7], gasification [8], and pyrolysis [9], hydrothermal liquefaction (HTL) is perhaps the most appealing.

## 2.2 Hydrothermal Liquefaction

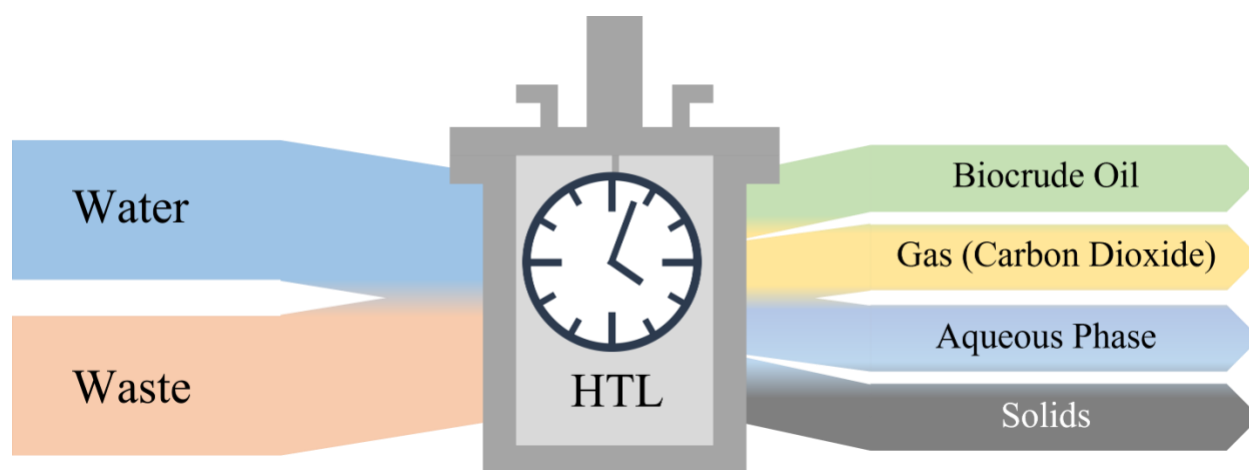


*Figure 3: Symbolic representation of HTL process*

Hydrothermal liquefaction (HTL) is a thermochemical process that uses moderate heat and pressure to convert wet organic feeds into energy-dense biocrude. Along with oil, HTL reactions produce aqueous, solid, and gas phase products, as shown in Figure 3. Optimal reaction conditions vary from feed to feed, but HTL reaction temperatures typically range from 523 to 647 Kelvin. Operating pressures typically range from 4 to 22 MPa [10]. HTL is a very versatile process for conversion of waste to biocrude: feeds can include food waste, biomass, plastic waste, sewage sludge, and other organics [10].

HTL is not the only process capable of converting waste to oil, but it has several important advantages over similar processes such as anaerobic digestion, gasification, and pyrolysis. Gasification and pyrolysis are similar processes that take place in reactive and inert environments, respectively [8, 9]. Unlike these two processes, HTL does not require dried feeds. Drying feeds – particularly waste feeds - is often expensive and impractical, giving HTL a clear advantage. Anaerobic digestion, while versatile and widely used in wastewater treatment,

requires lengthy residence times of 20 to 30 days [7]. While this is acceptable for large-scale operations, the relatively short residence time required for an HTL reaction, roughly one hour, allows for much more flexibility and modularity.

While the precise reaction mechanisms involved in an HTL reaction are ample and complex, the general scheme takes place in several identifiable steps. First, large organic structures present in the feed, such as lipids or cellulose, are depolymerized into smaller chains. These smaller chains further decompose into small, typically water-soluble organic molecules by mechanisms including dehydration, decarboxylation, and deamination. At HTL temperatures, subcritical or supercritical water disrupts hydrogen-bonding networks present in feeds, solubilizing small component molecules. Some quantity of these small organics continue to degrade into carbon dioxide and other product gases. However, most will begin to repolymerize into hydrocarbon chains, forming the most desired product: biocrude. As the reaction continues, the mid-sized hydrocarbons of the oil phase will continue to polymerize into the solid product, often referred to as char or coke: a vast network of highly crosslinked hydrocarbons [10]. Figure 4 illustrates this process.

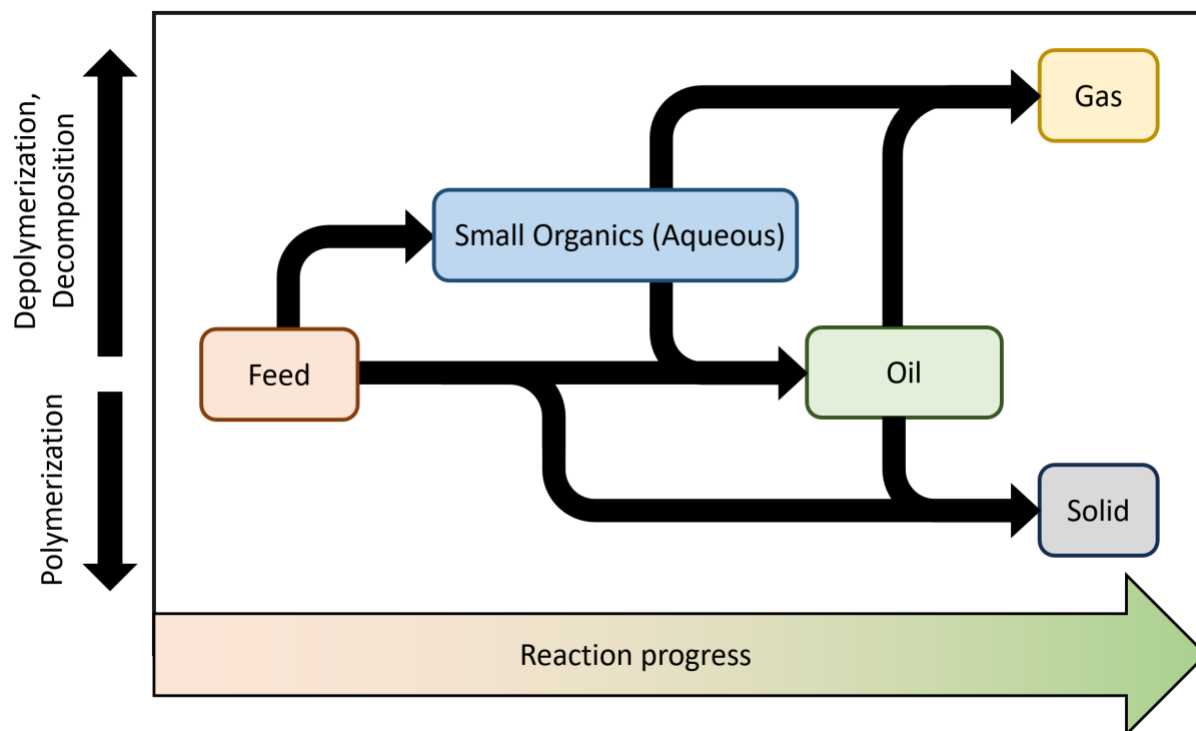


*Figure 4: Schematic representation of typical HTL reaction pathways. The feed decomposes into small organics and polymerizes into the solid phase. As the reaction progresses, small organics repolymerize into biocrude and solid and further decompose into gas [10]*

## 2.3 Co-Fed HTL

While single-feed HTL is a promising strategy for conversion of waste to energy, mixing various feeds for use in HTL reactions has been shown to improve biocrude yield by enabling chemical pathways not observed for single feeds individually [11, 12, 13]. Combining feeds for HTL may be beneficial for several reasons. Mixing feeds may allow for greater oil yield than would be expected from a simple linear interpolation between the oil yields of the two feeds individually. Feeds that would be non-viable for use in HTL on their own may suddenly be useful if the addition of a second feed increased biocrude output. Additionally, mixing feeds may

make low-cost feeds more productive and economically viable. The quality of the biocrude may also be improved by mixing of feeds, decreasing the need for costly upgrading.

The oil yield of hydrothermal co-liquefaction reactions rarely trends linearly between oil yields of the two individual feeds [12]. Typically, the new chemical behavior of the mixed feed HTL reaction produces some synergistic or antagonistic effect, sometimes depending on the ratio of the two feeds. While it is often difficult to predict the effect of mixing feedstocks, HTL of several combinations of mixed model compounds has been studied. Feeds for HTL generally fall under three categories: protein, lipid, and carbohydrate. Many feeds, such as food waste or sewage sludge, contain a mixture of compounds in these categories. Carbohydrates include the biomass components of cellulose, hemicellulose, and lignin.

One of the most notable observed synergistic effects occurs in mixed feed HTL of protein and carbohydrates. Mixing these feeds in HTL reactions has been shown to cause a significant synergistic effect on biocrude yield, particularly at higher ratios of protein to carbohydrate [11, 12]. This effect may be partially attributed to the Maillard reaction between reducing sugars and amino acids, from decomposed cellulose/hemicellulose and protein, respectively. Interestingly, at higher ratios of carbohydrate-rich green waste to protein-rich food waste, LeClerc et al. found that increased decarboxylation due to the greater cellulose content caused increased polymerization, causing, in turn, higher char formation and lower biocrude yields. Figure 5 elegantly illustrates this phenomenon [11]. The feeds and methods used in this study are very similar to those used in the study conducted by LeClerc et al., allowing for easy comparison of results.

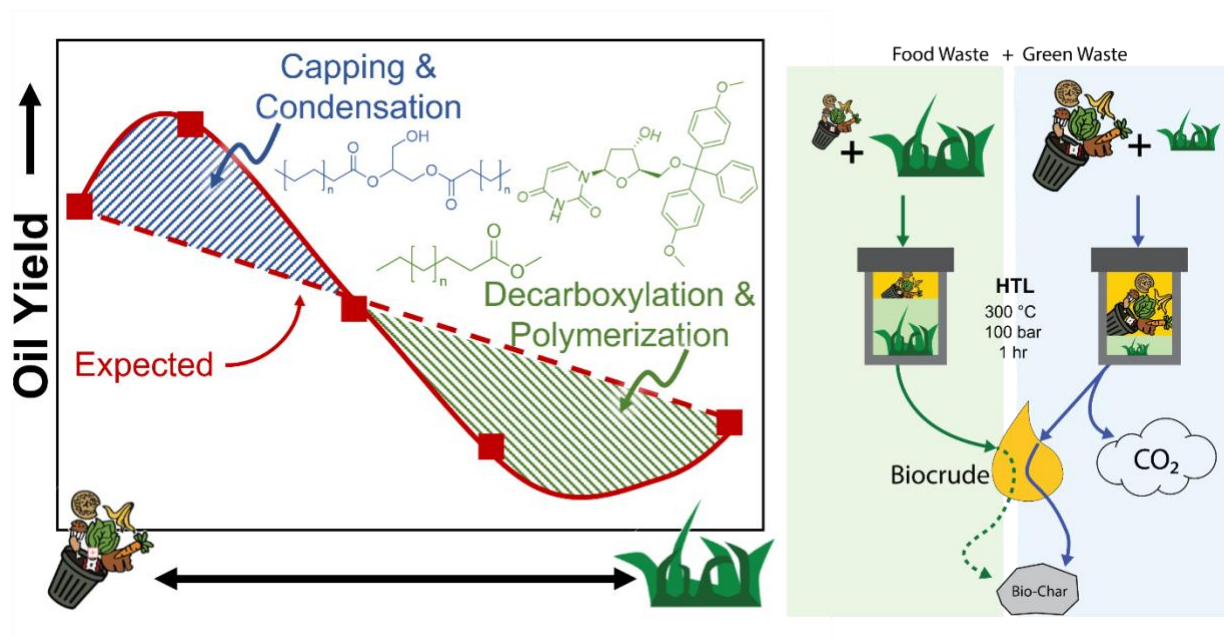


Figure 5: Illustration of synergistic and antagonistic effects observed for mixed feed HTL of biomass and food waste [11].

## 2.4 Food Waste and Lignin

The two feeds used in this study were kitchen food waste and CELF-derived lignin. These feeds were tested in HTL reactions individually, and at mass ratios of 25:75, 50:50 and 75:25. This section will briefly describe the origins, compositions, and other important properties of these feeds. The kitchen food waste was sourced from Coyote Ridge Correctional Facility in Connell, Washington. The waste was autoclaved on 03/20/2021, and shipped to WPI, where it has been stored in a freezer. The prison kitchen food waste (PKFW) is 53.9% carbohydrate, 18.6% lipid, and 21.7% protein by mass, as determined by biochemical analysis. It has a dry higher heating value (HHV) of 21.1 MJ/kg. Large facilities such as schools, hospitals, or correctional facilities are particularly attractive as feed source for biofuel production due to the

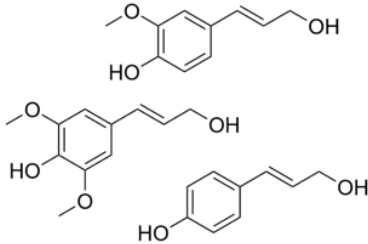
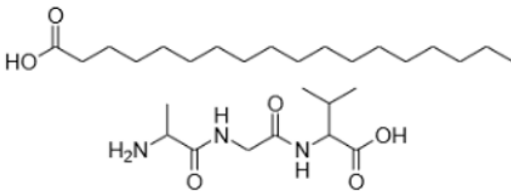
large volume and consistency of the food waste they produce. A high volume of waste available at a single point could decrease transportation costs for a biofuel production facility, and the consistency of the waste stream could allow for optimization of HTL conditions.

The lignin used in this study was originally isolated from green waste collected by Athens Services of City of Industry, California. This green waste was likely collected by Athens Services' organics recycling program for residential and commercial customers [14]. It is likely that the original waste supply contained some quantity of food scraps if the waste was collected from residential customers. Lignin was isolated from the cellulosic and hemicellulosic fractions of the green waste using co-solvent enhanced lignocellulosic fractionation (CELf) by researchers at the University of California Riverside. The lignin used in this study was processed at 180 °C for 30 minutes, with a solvent ratio of 2:1 THF to water. The CELf process will be described in more depth in the next section. Lignin is a vast, highly crosslinked biopolymer primarily composed of three monomers: trans-p-coumaryl alcohol, coniferyl alcohol, and sinapyl alcohol [15]. The relative compositions of these three components (particularly the ratio of sinapyl alcohol to coniferyl alcohol, reported as the S/G ratio) has a notable impact on the properties of the lignin itself. Several studies have been conducted on the effects of the S/G ratio on fuel production from lignin, which fall outside the scope of this study [16]. The isolated lignin was shipped to WPI, where it has also been stored in a freezer to limit degradation. The lignin used in this study has a HHV of 26.5 MJ/kg. Typical plant biomass is composed of roughly 50% cellulose, 20% hemicellulose, and 30% lignin by mass. Vast quantities of plant biomass is processed yearly to produce cellulose for use in manufacturing paper and other goods. Lignin is produced as a waste product of this process. The world produces approximately 100 million tonnes of lignin per year, making this a very appealing feed for biofuel production [17].



Images of both feeds can be found in Appendix A. The table below concisely summarizes some of the information presented in this section.

*Table 1: Origin, makeup, and typical molecular structures found in lignin and food waste [15]*

	Lignin	Food Waste
Origin	Athens Services City of Industry, CA	Coyote Ridge Correctional Facility Connell, WA
Chemical Makeup	Trans-p-Coumaryl alcohol Coniferyl alcohol Sinapyl alcohol [15]	Long-chain fatty acids Proteins Carbohydrates
Typical Components		

## 2.5 Cosolvent Enhanced Lignocellulosic Fractionation

The lignin used in this study was produced using cosolvent-enhanced lignocellulosic fractionation (CELf). During this process, plant biomass is first ground into small particles, less than one millimeter in size. The ground biomass is then pre-treated in a benchtop reactor with an acid catalyst (such as sulfuric acid) and a mixture of 1:1 to 7:1 of THF:water. The CELf pretreatment is carried out at a temperature in the range of 160 to 180 °C for 15 to 30 minutes. The cellulose-rich solid is then separated from the hydrolysate via vacuum filtration. This hydrolysate is then distilled to isolate the dissolved lignin, then purified by washing with water and filtration, then dried [18]. Figure 6 displays this process visually.

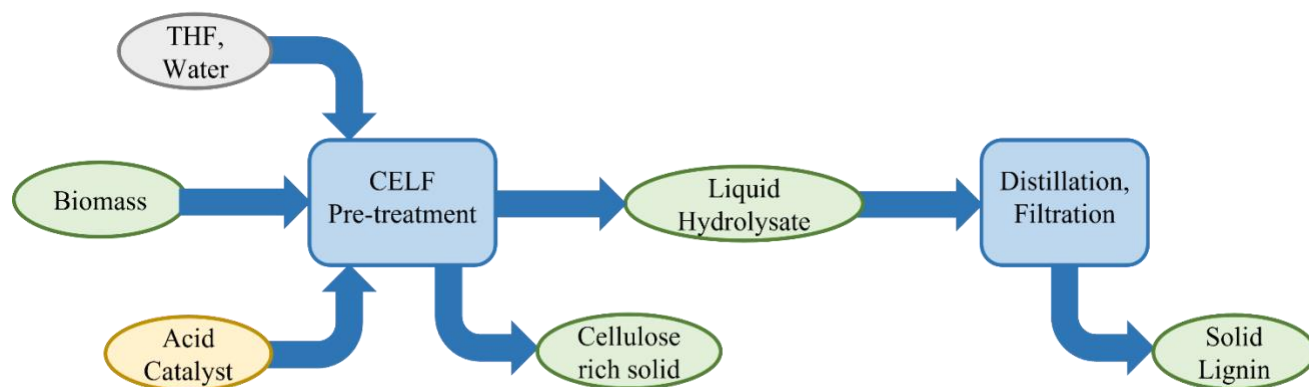


Figure 6: Schematic representation of CELF process for lignin isolation [18]

While the CELF process is effective at isolating high-quality lignin from plant biomass, it is not the dominant process used in industry for this purpose. Kraft pulping is widely used to separate cellulosic fibers from lignin in biomass. Using a heated solution of sodium hydroxide and sodium sulfide, the lignin is dissolved from the plant biomass in three main phases at different temperatures. After the completion of these three phases, the dissolved lignin is typically burned for energy [19]. Lignin produced by Kraft pulping is typically high in sulfur, unlike the sulfur-free lignin produced by the CELF process. Sulfur is undesirable as a component in fuels due to the negative environmental impact of its combustion products. This makes kraft lignin somewhat problematic for use in biofuels without expensive refining to remove sulfur. For this reason, CELF lignin is far more useful as a feed for HTL, despite its relative unpopularity as an industrial process.

## 2.6 Motivation

Both food waste and lignin are inexpensive, abundant, and energy-rich. Their disposal has a massive global environmental impact, the mitigation of which is a high priority for

minimizing carbon emission and other forms of pollution. As fossil fuel deposits dwindle and their use is decreased due to environmental concerns, the world is faced with a lack of energy-dense fuels, particularly for use in transportation. HTL has been shown to be an effective and economically viable method to transform waste into biocrude, which may be further refined into usable fuel. HTL of both individual feeds used in this study, food waste and lignin, has been successful. Studies have also shown that HTL of mixed feeds often results in unpredictable synergistic and antagonistic effects on oil yield and quality. Since the exact mechanisms of HTL are difficult to identify and fully understand, this finding opens the door to many mixed feed HTL studies on various mixtures of feeds. The goal of this study is to investigate the properties of HTL of combined food waste and lignin. Figure 7 shows the overall process investigated in this study.

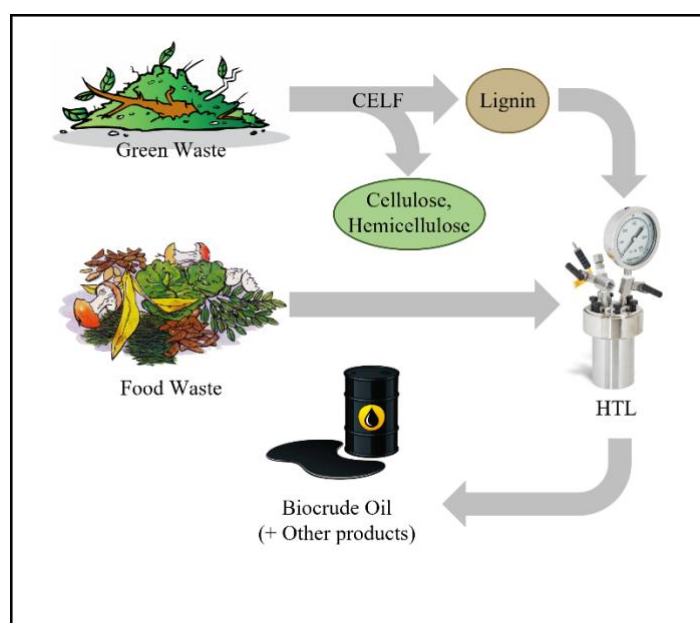


*Figure 7: Flow diagram for overall waste-to-energy process for HTL of food waste and lignin*

## 3.0 Methods

### 3.1 Hydrothermal Liquefaction: Setup

This section will describe the process of setting up and starting a hydrothermal liquefaction reaction. The procedure used in this study was based on methods described by LeClerc et al. [11]. A paper tracking sheet was used to record information for each reaction, a sample of which can be found in Appendix B. First, the desired masses of dry food waste and lignin were determined according to the desired feed ratio for the reaction. The water content of the frozen food waste was taken into account, and the desired mass of water to be added was reduced accordingly. Each reaction was completed with approximately 22.5 g of total dry feed and 127.5 g of water for a total reaction mass of 150 g. A 250 mL Parr benchtop reactor fitted with an impeller, rupture disc, pressure gauge, and two valves was used in this study. A PID controller was used to regulate the heating jacket. After recording the initial mass of the reactor bottom and head, the solid feedstocks were added to the bottom of the reactor. First, a wedge was used to break apart the frozen food waste. A large weigh boat was tared on a balance, then a spatula was used to scoop chunks of food waste into the boat until the desired mass was achieved. After adding the food waste to the reactor bottom, the weigh boat was weighed once more to account for residual mass left in the boat. The same process was then used to add the desired mass of lignin to the reactor bottom. Next, a beaker was tared on a scale and distilled water was added until the desired mass of water was reached. After pouring the water into the reactor, the mass of the beaker was measured once more to account for residual water.

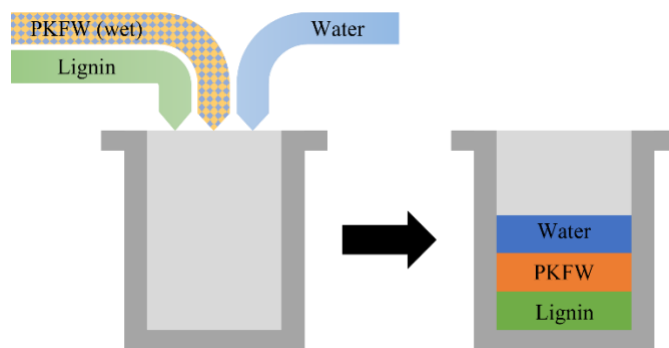


*Figure 8: Feed and water are added to the reactor in preparation for HTL*

Once the reactor bottom was loaded with the desired masses of feed and water, the reactor head was placed on top, and the total initial mass of the reactor (including bottom, head, feed, and water) was recorded. Next, the reactor was placed in a vice grip and a collar was attached, holding the reactor bottom and head together. The six bolts on the collar (three on each half) were tightened with a wrench. An additional metal collar was fitted around the main collar to ensure that the two halves could not separate during the reaction. The reactor was then placed into the benchtop reactor stand inside a fume hood. The impeller driveshaft was attached to the head of the reactor and cooling water tubes were attached to ports on the reactor head. The heating jacket was raised to cover the bottom of the reactor using a small jack. Images of the reactor setup may be found in Appendix A.

Next, the reactor was purged and pressurized with pure nitrogen gas. A high-pressure nitrogen gas line was attached to one of the valves on the head of the reactor and tightened with a wrench. The reactor was filled with nitrogen gas to a pressure of at least 900 PSI, then vented slowly into the fume hood. This process was repeated two additional times. After the third pressurization to 900 PSI, both valves of the reactor were closed, and the reactor was observed

for at least 60 seconds to check for leaks. After confirming that the reactor was properly sealed, the pressure was decreased to 300 PSI for the start of the run.

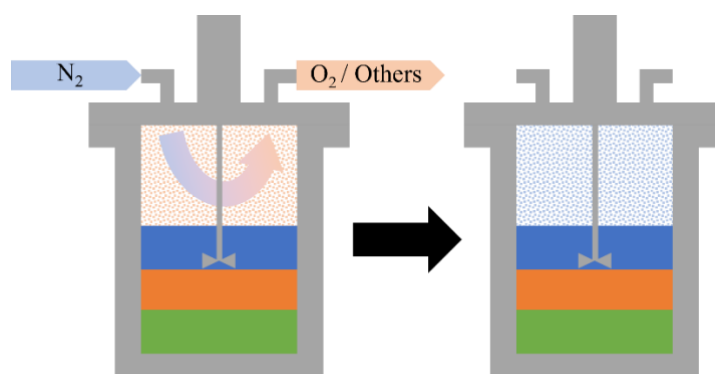


*Figure 9: The reactor is purged with nitrogen gas*

After pressurization, the heating jacket was switched on to begin the heat up process. The start time and initial pressure and temperature were recorded. Every reaction for this study was carried out at 300 °C, so the set point of the heater was set to 310 °C to decrease time required for heat up. Over the course of the heat up, the temperature and pressure of the reactor were monitored. As the reactor approached 300 °C, the controller set point was decreased to 300. Once the internal temperature of the reactor reached 300 °C, the internal temperature and pressure of the reactor were recorded, along with the reaction start time. Reactor heat up typically took about 40 minutes. Reactions were allowed to continue for one hour at 300 °C. The reactor temperature and pressure were monitored over the course of the hour-long reaction.

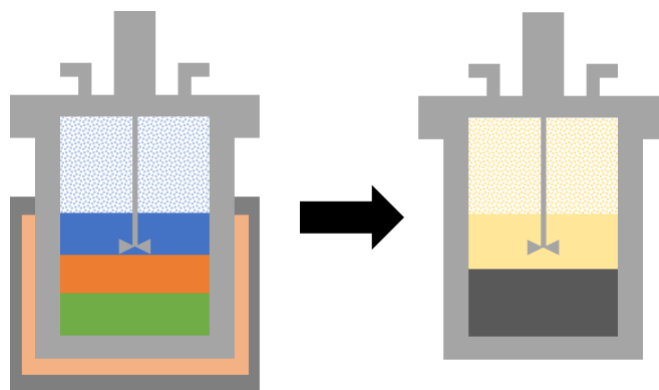


*Figure 10: The HTL reaction is completed, generating oil, solid, aqueous, and gas phase products*

### 3.2 Hydrothermal Liquefaction: Separations

The products of a HTL reaction separate into three distinct phases: gas, aqueous, solid, and oil. The gas developed by the reaction is primarily carbon dioxide, the mass of which is not directly measurable. Two methods may be used to estimate the mass of carbon dioxide generated. One way is to subtract the final reactor mass after the HTL reaction and degassing from the initial mass recorded prior to pressurization. While more direct, this method is imprecise, as the entire reactor weighs more than 10 kg, and the mass of gas produced is difficult to detect in comparison. Instead, the temperature and pressure measurements from after quenching may be compared to those taken before the start of heat up. Treating the headspace of the reactor as an ideal gas allows the number of moles of gas evolved in the reaction to be calculated. This method was used in this study due to its superior precision and consistency.

The other three phases may be measured more directly. The oil phase product of the reaction is hydrophobic, and clings to the solid phase. This allows for easy separation and measurement of the aqueous phase via vacuum filtration. While some moisture remains in the

solid and oil phases after filtration, this leftover water is quantified and added to the measured aqueous phase. The oil phase is extracted from the solid using acetone and may be measured directly after rotary evaporation. The solid phase may also be measured directly after drying.

Once one hour had elapsed since the reactor first reached 300 °C, the reaction was quenched using an ice bath. The heating jacket was switched off and lowered away from the reactor. Using a heat glove, the heating jacket was placed to the side, and a small metal bucket of ice water was placed on the jack and raised around the reactor bottom. Ice was also placed around the exposed reactor collar to hasten cooling. As the ice in the bucket melted, new ice was added as necessary. Once the internal temperature of the reactor was 40 °C or lower, the time, temperature, and internal pressure were recorded one final time. Quenching typically required about 10 minutes.

Once cooled, the reactor was depressurized in the fume hood by slowly opening one of the valves. The reactor was then removed from the benchtop reactor stand, and the collars were removed with a wrench. The final total reactor mass was then measured and recorded. Paper towels were used to dry the exterior of the reactor before weighing, if necessary. The reactor was then brought back to the fume hood and the seal between the head and bottom was broken in preparation for separations. A small wedge was occasionally used to pry the reactor head and bottom apart if they were stuck.



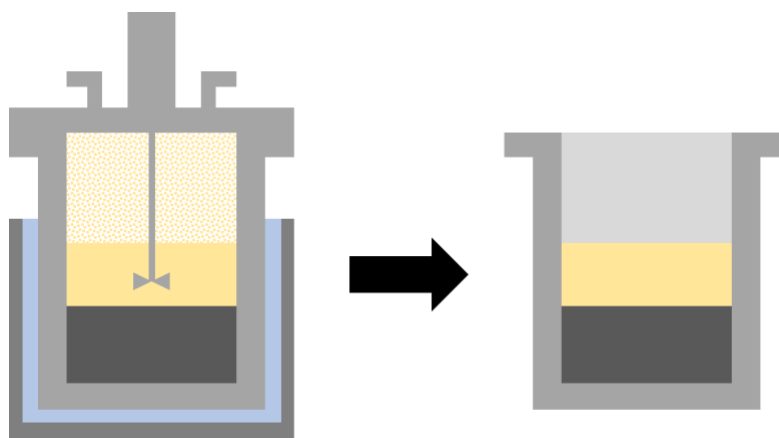


*Figure 11: The reactor is cooled in an ice bath, then the reactor head is removed after depressurization*

Next, the aqueous phase was separated from the oil and solid phases by vacuum filtration. The mass of a filtering funnel with a small rubber stopper and 90 mm diameter filter paper were recorded. To accurately measure the mass of aqueous phase, the mass of a 250 mL vacuum flask was also recorded. A stand and clamp were used to hold the flask in place while a rubber tube attached to a vacuum pump was fitted to its stem. The filtering funnel was placed into the flask, and the vacuum pump was switched on.

The reactor head was lifted slowly from the bottom, and care was taken to avoid spilling any of the reactor contents. Oil typically accumulated on the impeller, so a small spatula was used to scrape its shaft and blades. Occasionally (particularly for the reactions with more lignin feed), the solid phase accumulated in brittle deposits in the impeller and reactor walls. The spatula was also used to break up these deposits. Once thoroughly scraped of water and oil, the reactor head was placed to the side. The spatula was used to scrape accumulated oil and solids from the walls and bottom of the reactor and agitate the mixture. Large chunks of solid were broken up where possible. After fully agitating the reactor contents, the contents of the reactor

were poured into the filtering funnel. Completing this task in one step is ideal to minimize residuals left in the reactor bottom. The spatula was used to thoroughly scrape the walls of the reactor and get all of the contents of the reactor into the filtering funnel. While some water will inevitably remain in the reactor bottom after scraping, this residual water should be minimized.

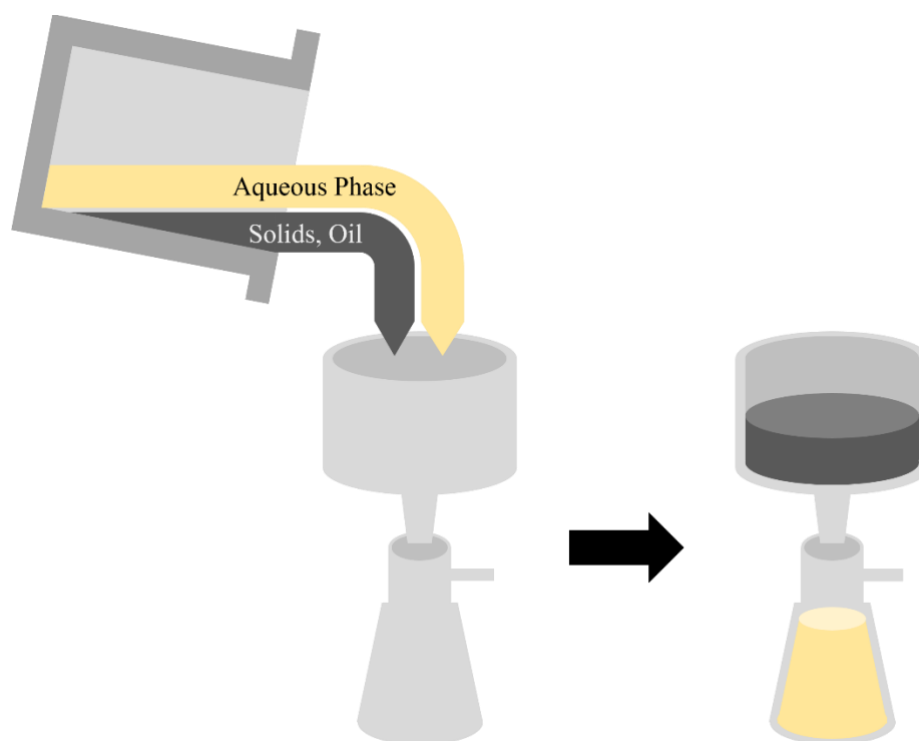


*Figure 12: The solid and aqueous products of the HTL reactions are separated via vacuum filtration*

The vacuum filtration was allowed to continue until the contents of the filtering funnel appeared dry and water was no longer dripping from the bottom of the funnel into the vacuum flask. Once dry, the vacuum pump was switched off and the funnel and stopper were removed from the flask. The vacuum flask was reweighed to determine the mass of the aqueous phase. The aqueous phase was yellow-orange in color and transparent. Taking care not to spill the contents, the mass of the filtering funnel including the stopper, filter, and contents of the funnel

were recorded. While this measurement was not used in subsequent analysis, it may be used for confirmation or troubleshooting potential issues.

Next, the oil was extracted from the solid phase using acetone. A 1 L vacuum flask was clamped to the stand, and the rubber tube to the vacuum pump was fitted to the stem. Roughly 500 mL of acetone (Fisher Chemical,  $\geq 99.5\%$ ) was poured into a beaker to be used in the extraction. The bottom of the reactor was filled halfway with this acetone, and the spatula was used to scrape walls of the reactor, releasing any oil into the acetone. Since oil often accumulated on the impeller and head of the reactor, the head must be washed with this acetone. The impeller was lowered into the acetone, and the spatula was used to scrape it. Once the impeller was clean of oil, the head was tilted, and a squeeze bottle of acetone (containing used acetone) was used to spray acetone over the bottom surface of the head, using the reactor bottom to collect the acetone and oil that ran off. This ensures that minimal oil is lost to the head. The acetone squeeze bottle was used sparingly, as the acetone inside likely contained trace amounts of water.

Once the head and impeller were clean of oil, they were once again set to the side. After agitating the contents of the reactor bottom once more, the liquid was poured quickly into the filtering funnel. The reactor bottom was then filled with acetone at least one more time and scraped. The contents were again poured into the filtering funnel. After this second wash, most of the oil had been extracted from the solid phase. Acetone was poured into the funnel repeatedly until the liquid dripping from the bottom of the funnel into the flask ran clear. Additional fresh acetone was added to the beaker as necessary. While washing the solid phase, the spatula was used to agitate the contents of the filtering funnel and gently break up large chunks of solid to aid in the extraction. Once the solid was completely washed, the vacuum filtration was allowed to continue for several minutes to fully dry the solid phase of acetone. Evaporation of acetone from

the vacuum flask is allowable since the mass of acetone is never recorded. Extractions typically required between 500 mL and 1 L of acetone.

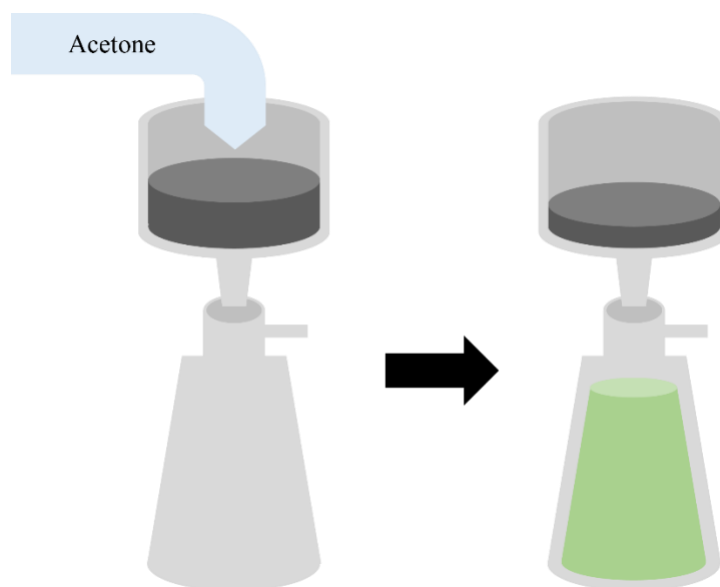


*Figure 13: The solid filter cake is washed with acetone, removing the biocrude product*

Once the solid contents of the filtering funnel were completely dry of acetone, the funnel, stopper, filter, and solid phase were weighed for the third time. To determine the water content of the solid phase, the solids were dried at 60 °C for at least 12 hours. Immediately after weighing the filtering funnel, its contents, and the stopper, the solid phase was transferred to a previously weighed 50 mL beaker. This beaker was weighed once more, then moved to a drying oven. The difference in mass after drying was used to calculate the water content of the solid phase, which is non-negligible.

Next, the oil was separated from the washing acetone by rotary evaporation. A 1 L round-bottom flask was weighed, then the acetone/oil solution was poured into it. The round-bottomed flask was attached to a rotary evaporator, and partially submerged in a water bath at 50 °C. The solution put under a vacuum of 370 mbar, and slowly rotated in the water bath. After

evaporation, only oil and residual water remained in the round-bottom flask. The exterior of the flask was dried, and re-weighed to determine the mass of oil produced. The contents of the flask were then poured and scraped into a small vial for storage and further characterization. The extracted oil often contained significant amounts of water, particularly for the reactions with more lignin feed. In some cases, the extract contained enough water to cause phase separation with the oil. While the oil was not dried, the water was quantified later using Karl Fischer titration.

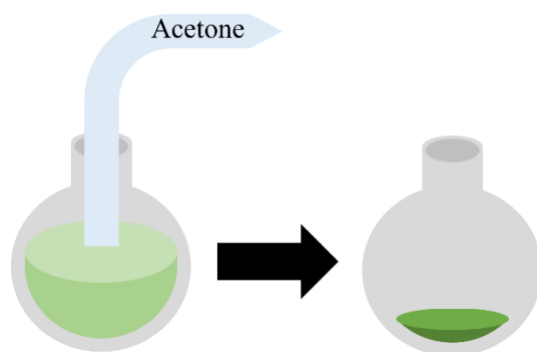


*Figure 14: Rotary evaporation is used to isolate the oil product from acetone*

### 3.3 Elemental Analysis

One of the most important characterizations of the products of HTL reactions used in this study was elemental analysis. Samples of the undried oil phase product, dried solid phase product, and both feeds were sent to Midwest Microlabs (Indianapolis, IN) for CHN analysis. This analysis yielded the fractional mass composition of carbon, hydrogen, and nitrogen in the samples. The remainder of the mass of each sample was assumed to be oxygen. According to the Midwest Microlabs website, samples are combusted in pure oxygen at 990 °C,

and the resultant product gases (water, carbon dioxide, and nitrogen) are quantified. Air-sensitive samples may be loaded under pure nitrogen in a glove box, though this treatment was not required for any of the samples in this study [20]. An example elemental analysis report may be found in Appendix B.

First, the fraction of carbon in each of the feeds (as well as the mass fraction of water in the frozen food waste) was used to calculate the total carbon entering the reaction. This value would later be used to calculate carbon yields. The fractions of carbon, hydrogen, and nitrogen in each product sample were then used to determine dry basis carbon yields and heuristic higher heating values. For the dried solid samples, the carbon yield was relatively easy to calculate using the elemental data: the carbon content of the solid was multiplied by the mass of dry solid product, then divided by the total feed carbon. For the oil phase products, the water content of the oil had to be taken into consideration when calculating carbon yield. Oil moisture was determined using Karl Fischer titration, described in section 3.5. The water content of the oil caused an artificially high oxygen elemental composition result, and, by extension, an artificially low carbon content result and carbon yield. To address this, the carbon content of the wet oil was divided by the moisture content of the oil, yielding an adjusted carbon content for the dry oil. The same transformation was done for nitrogen. For hydrogen and oxygen, the composition of the water was taken into account and subtracted from the total hydrogen and oxygen measurements before scaling up. Sections 4.3 and 4.4 show the results of the elemental analysis and carbon balance.

The elemental composition of the oil was used to estimate its higher heating value (HHV). Typically, HHV is measured using bomb calorimetry, but it may be accurately estimated using heuristic equations such as the Dulong equation [21], shown below.

$$HHV \left( \frac{Kcal}{kg} \right) = (78.31 * \%C) + 359.32 * \left( \%H - \frac{\%O}{8} \right) + (22.12 * \%S) + (11.87 * \%O) \\ + (5.78 * \%N)$$

This widely-used equation was used in this study to estimate the HHV of the dry biocrude using their elemental compositions of carbon, hydrogen, oxygen, and sulfur. A more novel heuristic equation, proposed by Klaus Schmidt-Rohr, was also used to estimate the HHVs of the oils in this study [22]. This equation relies on the principle that combustion reactions yield approximately 418 kJ per mole of oxygen gas consumed. Therefore, one may estimate the number of moles of oxygen gas required for a reaction (by multiplying the elemental molar compositions of a material by stoichiometrically-dictated factors), and multiply this value by -418 kJ to accurately estimate the enthalpy change of combustion. This second equation, which requires molar rather than mass fractions, is presented below:

$$\Delta H \left( \frac{kJ}{mol} \right) = -418 \frac{kJ}{mol} * [\%C + (0.3 * \%H) - (0.5 * \%O)]$$

Since elemental analysis data is reported in mass fractions instead of molar fractions, the equation was modified for use in this study:

$$HHV \left( \frac{MJ}{kg} \right) = 418 * \left[ \frac{\%C}{12 \frac{g}{mol}} + \left( 0.3 * \frac{\%H}{1 \frac{g}{mol}} \right) - \left( 0.5 * \frac{\%O}{16 \frac{g}{mol}} \right) \right]$$

Values obtained from the Dulong equation and the equation proposed by Schmidt-Rohr were found to agree to within 3% of each other. Estimated HHVs from both equations may be found in section 4.4.

### 3.4 Total Organic Carbon Analysis

The compositions of the solid and oil phase products were determined by elemental analysis, and the carbon content of the gas was estimated using the ideal gas law and the assumption that all evolved gas was carbon dioxide. This leaves only the carbon content of the aqueous phase to be analyzed to complete the carbon balance for the HTL reaction. Aqueous carbon was quantified using total organic carbon (TOC) analysis, completed with a Shimadzu Co. TOC-L series analyzer. The TOC-L instrument uses catalytic combustion at 680 °C [23] to quantify organic carbon (OC); a sample is evaporated and subsequently combusted in the presence of a metal catalyst such as platinum, copper, iridium, or nickel [24] to achieve complete combustion of OC. Catalytic combustion is considered one of the quickest and most reliable methods for determination of organic carbon content [24]. However, all inorganic carbon (IC) must be removed from the sample or dissolved prior to analysis. To accomplish this, samples were pre-treated with acid using a method similar to that used by Cheng et al. [25]. The instrument was calibrated prior to each batch of samples with a series of four diluted potassium hydrogen phthalate (KHP) standards. Both the pre-treatment and standard preparation will be described in this section.

Samples were typically prepared in large batches as TOC analysis requires a relatively involved setup. For each sample, the required materials were one 3 mL syringe, one 45 micron filter (to be fitted to the end of the syringe), one 1 dram vial, one rubber topped vial, and one 100 mL volumetric flask. Each of the four standard solutions required one 100 mL volumetric flask and one rubber topped vial. First, all glassware to be used was washed with hydrochloric acid and rinsed with deionized water at least four times to eliminate all carbon from the glassware. Next, the aqueous phase was filtered. For each sample, the plunger of a syringe was removed,



and a filter was fitted to the tip. The syringe and filter were held over an open 1 dram vial as approximately 1 mL of aqueous phase sample was poured into the top of the syringe. The plunger was then used to press the rest of the sample into the vial.

Next, each of the volumetric flasks were filled with approximately 50 mL of deionized water from an acid-washed beaker. This prevents direct contact between the sample and the concentrated acid, which are added next. A micropipette was then used to add 15  $\mu\text{L}$  of each filtered aqueous phase sample to its respective flask. Micropipette tips were changed between samples. Using a larger micropipette tip, 1.0 mL of 6 M hydrochloric acid was then added to each flask. Once each flask contained the necessary quantities of sample and hydrochloric acid, the volumetric flasks were filled to the line using a Pasteur pipette, capped with parafilm, and inverted at least 20 times to ensure complete mixing. Once fully mixed, the flasks were uncapped and approximately 30 mL of solution was poured from each flask into a labeled septum vial.

KHP standard dilutions were prepared using a similar method. It was occasionally necessary to prepare a new KHP standard solution of 1000 ppm OC with which to make standard dilutions. The procedure for preparing this solution will be briefly described here. First, approximately 0.75 g of KHP powder (Sigma-Aldrich, ACS reagent) was dried in an oven at 103-110  $^{\circ}\text{C}$ . After 30 minutes, the sample was weighed every 5 minutes until the mass was constant, indicating complete drying. Exactly 0.5314 g of dried KHP was then weighed, then added to an acid-washed 250 mL volumetric flask. The flask was then filled to the line with deionized water, capped with parafilm, and inverted at least 20 times to ensure complete dissolution and mixing. The standard solution was then stored in an amber bottle, labeled with

the date of preparation. Standard solutions were refrigerated and discarded after one month to ensure accuracy of standards.

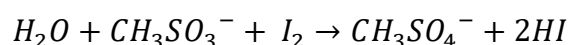
Four standard dilutions, with OC concentrations of 0 ppm, 2 ppm, 6 ppm, and 10 ppm were prepared and run before each batch of aqueous phase samples to calibrate the instrument. To prepare these samples, four acid-washed 100 mL volumetric flasks were filled partially (~50 mL) with deionized water from an acid-washed beaker. A micropipette was used to add 0.2 mL, 0.6 mL, and 1.0 mL of the standard 1000 ppm KHP solution into three different flasks. Next, 1.0 mL of 6 M hydrochloric acid (Fisher, 5.95-6.05 M) was added to each of the four flasks. All four flasks were filled to the line with deionized water, capped with parafilm, and inverted at least 20 times each to ensure complete mixing. Once mixed, the flasks were uncapped and approximately 20 mL of solution was poured from each flask into a rubber-capped vial marked with the corresponding OC concentration in ppm.

All sample solutions and standard dilutions were then transported across campus from Goddard Hall to Kaven Hall for TOC analysis. The TOC instrument was started, and the furnace began heating up to the desired 680 °C. Samples were added to the auto sampling tray and their information was entered into the program. The user ensured that the instrument had proper levels of all necessary fluids and proper flow of nitrogen. Once the instrument was initialized, the proper method was chosen, and the analysis was started. The instrument used the four standard solutions for calibration before moving on to the aqueous samples. An example TOC report including calibration can be found in Appendix B.

### 3.5 Karl Fischer Titration

As mentioned in section 3.3, the moisture content of the oil phase products must be quantified before the carbon balance can be completed. In this study, oil moisture was quantified by Karl Fischer titration, using a Mettler Toledo Titrator EasyPlus Easy KFV [26]. This method was first described by Karl Fischer in 1935 and has since become one of the most-commonly used and thoroughly reviewed methods for determination of water content. While the titration may be carried out manually, automatic titrators (such as the one used for this study) expedite the process. The chemistry of the reaction and the procedure used to carry out the titration will be briefly described here.

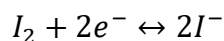
The Karl Fischer titration uses a solution of iodine, sulfur dioxide, and pyridine in methanol as the titrant, also known as the Karl Fischer reagent. Several reactions take place within the reagent, resulting in the formation of mesylate ions. As the titrant is added to a solution containing water, the iodine is rapidly converted to iodide ions according to the following reaction [27]:



As the titration proceeds, iodine concentration in the solution is negligible. However, once all water in the solution has been consumed by the reaction, further addition of titrant will introduce iodine into the solution. A detectable concentration of iodine in the solution indicates a complete titration.

Several methods exist to determine the end of the Karl Fischer titration. The electrochemical method, used in this study, is one of the most popular. Two electrodes are suspended in the solution, and a small potential is applied across the electrodes. While the

titration is in progress, there will be no current flow between the electrodes. As soon as the titration is completed, a small concentration of iodine appears in the solution, facilitating electrochemical conversion of iodine to iodide ions according to the following reaction [27]:



This reaction causes current to flow between the two electrodes, allowing the end point of the titration to be determined. The water content of the sample may then be calculated from the mass of sample added and quantity of titrant used to complete the titration.

Operation of the Mettler-Toledo Easy PlusEasy KVF was, true to its name, easy. First, approximately 0.2 g of biocrude was added to a 1 dram vial. The oil was mixed thoroughly prior to addition to the vial to ensure that the moisture was thoroughly distributed through the sample. Next, approximately 2 g of methanol (Fisher Chemical, HPLC grade  $\geq 99.9\%$ ) was added to the vial from a larger vial that was capped between uses. The vial was then capped and inverted repeatedly until the oil was fully dissolved. Next, one mL of oil/methanol solution was drawn into a 2 mL syringe equipped with a 3 1/8 inch needle. The syringe was then weighed. Once the instrument had reached equilibration, approximately one third of the contents of the syringe was injected into the titration vessel through a rubber septum, and the titration was started. The syringe was then re-weighed to determine the mass of oil/methanol solution injected into the vessel. This mass was entered into the instrument, which then reported the water content of the oil/methanol solution once the titration was complete. This process of injecting, weighing, and entering in the injected mass was repeated three times for each sample. Once all samples had been analyzed, the water content of the methanol was determined. A sample of the pure methanol from the larger vial was analyzed using the same procedure used for the oil samples. The water content of the methanol was typically negligible.

The water content of the oil was calculated by dividing the reported moisture of the oil/methanol solution by the dilution factor of oil in the solution. This value was used to determine the mass of dry oil produced in the reaction, which was then used to complete the carbon balance. A plot of the oil moisture content as a function of feed ratio may be found in section 4.2 of the results. A sample Karl Fischer titration run sheet may be found in Appendix B.

### 3.6 Gas Chromatography with Mass Spectrometry

The molecular compositions of oils were compared using gas chromatography with mass Spectrometry (GCMS), as done by LeClerc et al. [11] Analysis was completed using a Shimadzu GCMS-QP2010 SE equipped with a Shimadzu AOC-20i autoinjector. GCMS is a versatile and sensitive technique for compound identification which is widely used across different disciplines. The technique, which will be briefly described here, relies on a thin heated column to separate molecules, typically on the basis of molecular mass. A sample is injected into the head of the GC column and a flow of helium gas helps molecules travel through the length of column to the detector. Smaller molecules travel through the column more quickly than large molecules.

As molecules exit the column, they are passed to a mass spectrometer and bombarded with electrons. This causes the molecules to disintegrate into charged fragments which are then characterized by their mass to charge ( $m/z$ ) ratio. The spectrum of  $m/z$  signals recorded from an ionized molecule form an identifiable fingerprint which may be compared to libraries of known spectra to identify the original molecule [28].

To prepare samples for GCMS, a clean spatula was used to thoroughly mix oil samples then deposit approximately 0.02 g of oil sample into a 1-dram vial. The mass of oil sample was

recorded. Next, acetone (Fisher,  $\geq 99.5\%$ ) was added dropwise into the vial to prepare a 1 wt% oil solution. The final mass of the solution was also recorded.

The samples were filtered prior to injection on the GCMS. The plunger of a 3mL syringe was removed and set to the side, plunger side up to avoid contamination. A 45 micron filter was fitted to the tip of the syringe, and  $\sim 1.5$  mL of well-mixed oil/acetone solution was poured into the top of the syringe. The solution was then pressed into a 2 mL Shimadzu GC vial and the lid was secured. A sample of the acetone solvent was also prepared for validation.

Each sample was tested using the same method. Samples were injected at a split ratio of 10 and purge flow of 3 mL/min. To improve separation for volatile components, the column was initially held at 35 °C for the first 4 minutes after sample injection. The column temperature was then ramped up to 290 °C at a rate of 5 degrees per minute, then held isothermally for 40 minutes. The high temperature allowed heavier components of the oil to pass through the length of the column. Molecules were identified using the NIST database for m/z spectra.

### 3.7 Safety Considerations

Hydrothermal liquefaction reactions require potentially dangerous temperatures and pressures. To ensure safety for the operator and other members of the lab, multiple precautions were taken. While in the lab, researchers used proper personal protective equipment including long pants, non-open toed shoes, goggles, and gloves at all times. Lab coats were used as necessary. Most of the procedure was carried out in a fume hood including the HTL reaction, vacuum filtration, and rotary evaporation. All waste was stored in closed bottles with secondary containment to await proper disposal.

Before each reaction, the reactor was inspected for visible signs of wear or corrosion. The seal between the reactor bottom and head was inspected and trimmed or replaced as necessary. After loading feedstocks, the reactor was pressurized to at least 900 PSI and allowed to sit for at least 60 seconds to check for leaks. Over the course of the heat up and reaction, the head of the reactor was cooled with flowing water, and the internal pressure was monitored. In case of over pressurization, the reactor is outfitted with a rupture disc facing the rear of the fume hood. The reactor was allowed to cool to at least 40 °C after the reaction to avoid potential burns.

## 4.0 Results and Discussion

### 4.1 Mass Yields

Figure 15 shows the average mass yield for each of the four product phases for varying feed ratios. Both prison kitchen food waste (PKFW) and lignin feeds were evaluated for their HTL performance individually and at ratios of 25:75, 50:50, and 75:25.

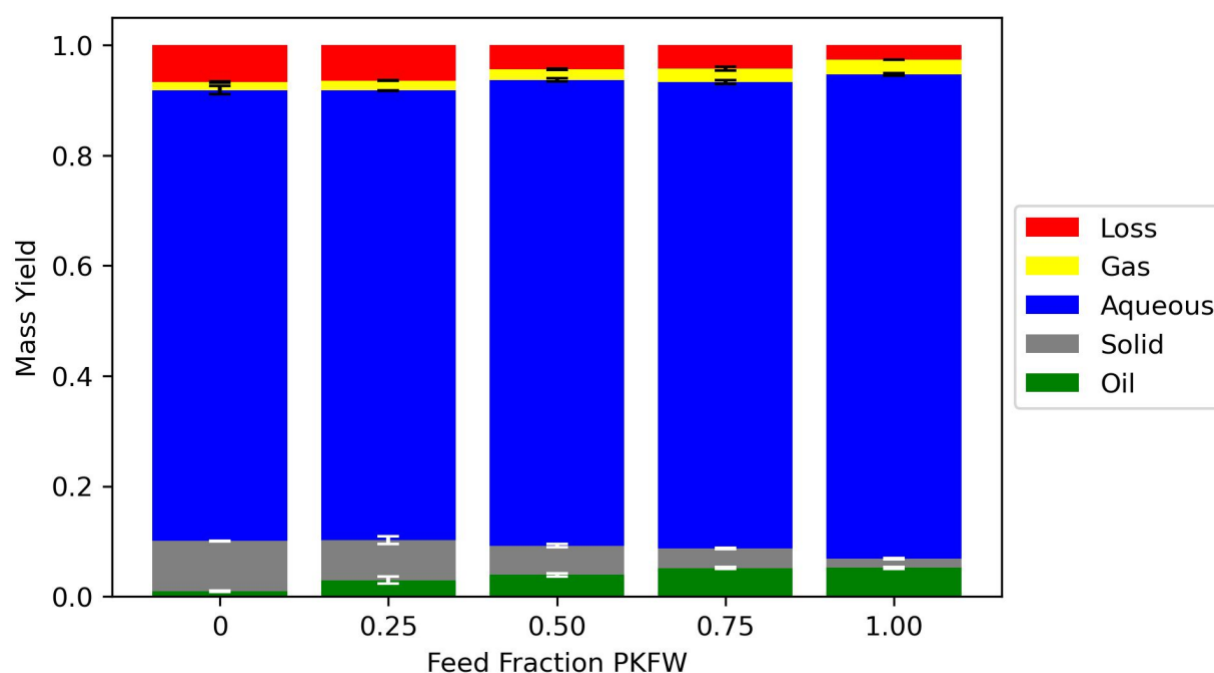


*Figure 15: Average mass yields observed for each product phase as a function of feed fraction PKFW. Ratios range from 0% PKFW feed on the left to 100% PKFW feed on the right. Error is reported as +/- one standard deviation for at least two trials for each ratio.*

Each trial shows a total average mass yield of over 90%, indicating that there was no significant mass loss during the reaction and separation processes. Error for each category is >1%, which demonstrates the reproducibility of the data. The aqueous phase contributed the majority of the mass yield for each trial. Since HTL reactions take place in an aqueous



environment, water makes up the bulk of the mass in both the products and reactants. The aqueous phase mass yield includes water remaining in the oil and solid phases after separations. While this plot is helpful to visualize the raw product distribution from the HTL reactions, a more detailed approach is necessary for understanding the organic partitioning from these reactions. A table containing values used to construct this plot may be found in Appendix C.

## 4.2 Moisture Content

The oil phase often contained a notable quantity of water. The oils produced from reactions with a low percentage of PKFW feed (0% and 25%) particularly suffered from this problem. Figure 16 below shows the moisture content of biocrude produced from each feed ratio. The higher error seen in the moisture of oils from the 0% and 25% PKFW reactions may be attributable to inconsistent sampling of the biphasic mixture of oil and water. The single-phase oils produced by the 50 - 100% PKFW reactions had more reproducible moisture measurements.

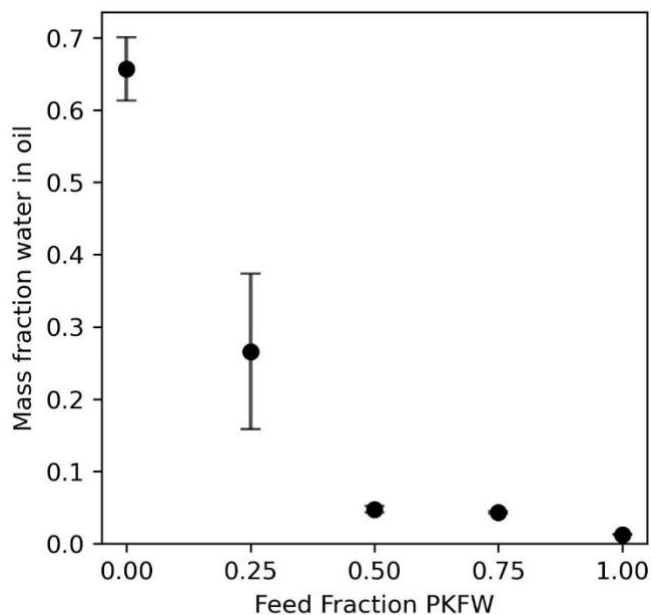


*Figure 16: Average oil moisture content as a function of feed fraction PKFW. Oils with a lower PKFW feed fraction had moisture contents up to 66%.*

The cause of the high water content of the 0% and 25% oils was not fully investigated, but there are several factors which likely contributed. These reactions typically had lower oil yields and higher solid yields. The solid phase is known to trap water, even after vacuum filtration. It is likely that water trapped in the solid phase was released by the acetone washing step and remained in the final oil after rotary evaporation. The high solid yield would allow for more water to be trapped after filtration, and the low oil yield would make the residual water more significant in comparison. It is also possible that the oil produced from HTL of lignin is more hydrophilic due to its composition. The monomers of lignin, trans-p-coumaryl alcohol, coniferyl alcohol, and sinapyl alcohol, are generally more hydrophilic than the components of food waste. While components of the original feed are not necessarily preserved during HTL, their structures will have an impact on the biocrude produced by the reaction.

### 4.3 Carbon Content

The ratio of feeds used for each reaction had a small effect on the compositions of the oil and solid products. Elemental compositions of both oil and solid product phases were obtained from Midwest Microlabs. Figure 17 below shows the elemental composition of the dry-basis oils as a function of feed ratio, and Figure 18 shows the elemental composition of the dried solids, also as a function of feed ratio.

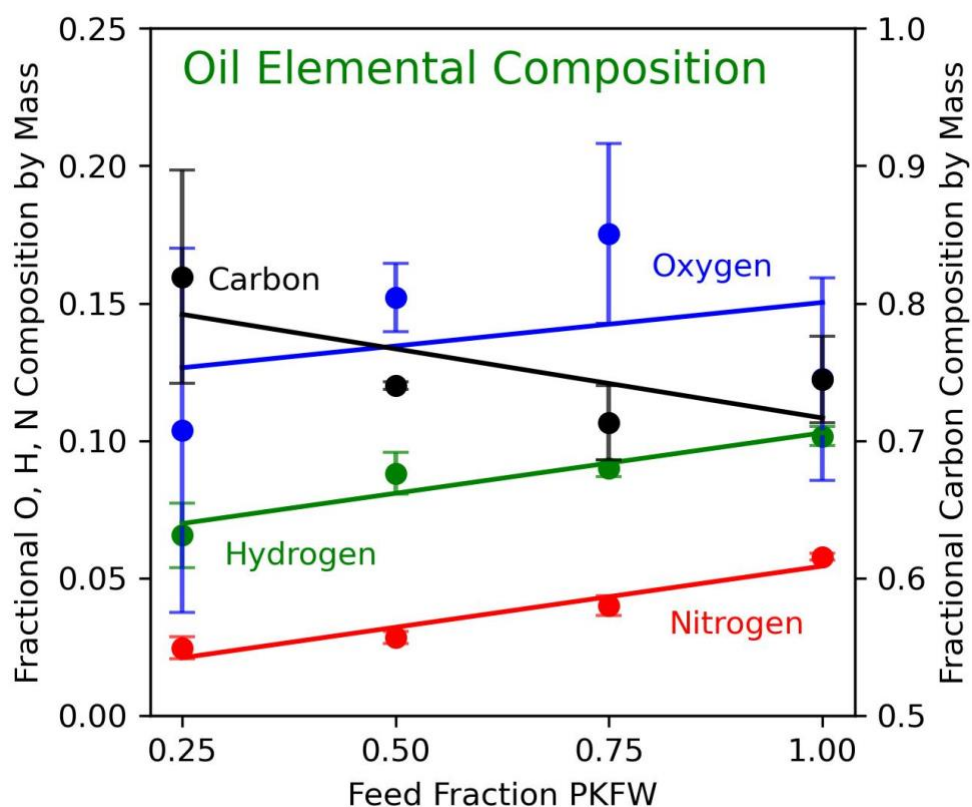
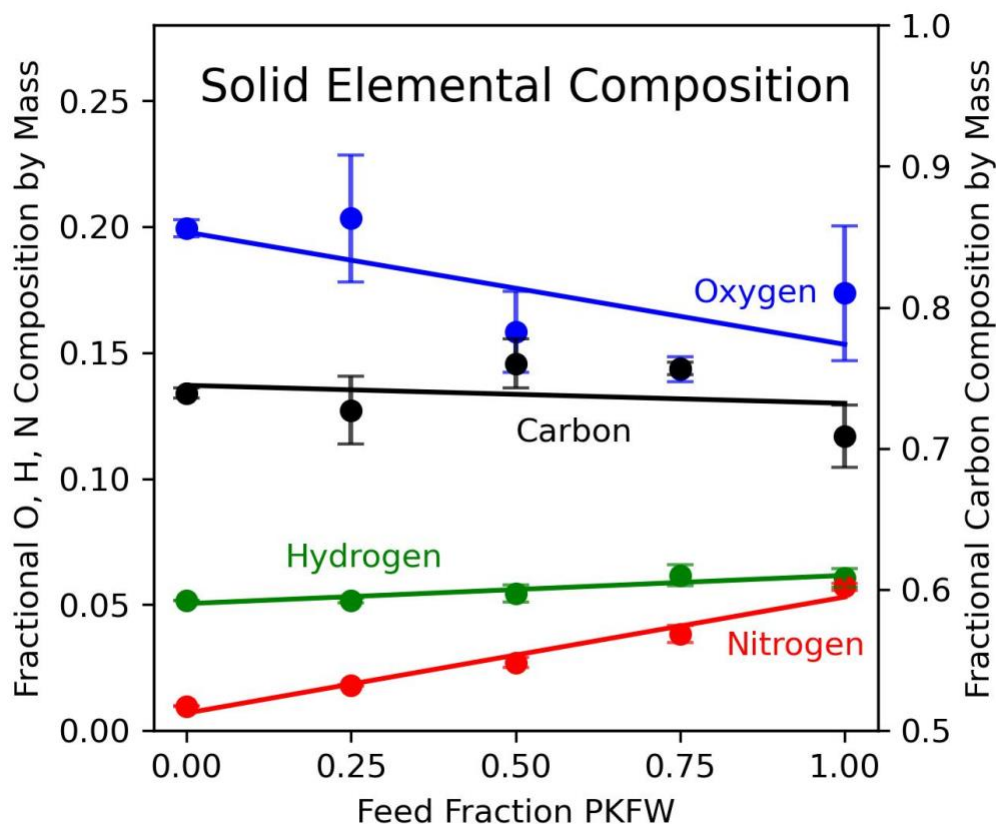


Figure 17: Moisture-corrected average elemental compositions for oils produced at various feed ratios. Carbon content is described by the y axis on the righthand side of the plot. Data for oils produced with 0% PKFW feed are omitted due to high moisture content.



*Figure 18: Moisture-corrected average elemental compositions for the solid product phase of mixed feed HTL reactions with various feed ratios. Carbon content is described by the y axis on the righthand side of the plot.*

Nitrogen content increased linearly in both oil and solid products for higher PKFW feed ratios, suggesting that nitrogen content is due to mixing effects. Hydrogen content also followed a slightly positive linear trend across feed ratios. Increased PKFW feed ratios generally led to greater partitioning of oxygen into the oil instead of the solid phase. At feed ratios of 50% and 75% PKFW, the oil had a slightly lower carbon content and slightly higher oxygen content than would be expected from mixing effects between the two feeds. It is possible that interaction between the two feeds in this range of ratios promotes polymerization, increasing the carbon content of the solid product, as observed by LeClerc et al. [11]. However, this trend is not

observed in the relative carbon yields of the oil and solid products and the deviations from linear behavior observed in Figures 17 and 18 are minimal. While novel chemical pathways may be altering the elemental compositions of the oil and solid products, the effects are insignificant to carbon yield. Further investigation would be required to fully understand the impact of feed ratio on elemental composition.

It should be noted that the data for the 0% PKFW oil composition was not included in this plot due to its extremely high measured moisture content. When the elemental composition of the oil was corrected to account for this water content, the calculated oxygen content was less than zero. This may suggest that the oil has a lower real moisture than that determined by KF titration. This is likely due to inconsistent sampling for moisture testing. However, the observed trend of consistent elemental compositions holds true for oils produced by the remaining four feed ratios. The low standard deviations observed for these trials suggests good reproducibility. Tables of elemental composition data for both the oil and solid phases may be found in Appendix C.

The moisture-corrected elemental composition of the oil was also used to estimate its higher heating value (HHV). Figure 19 shows the expected HHV in MJ/kg for oils produced from each feed ratio aside from 0% PKFW, which was omitted for reasons already discussed.

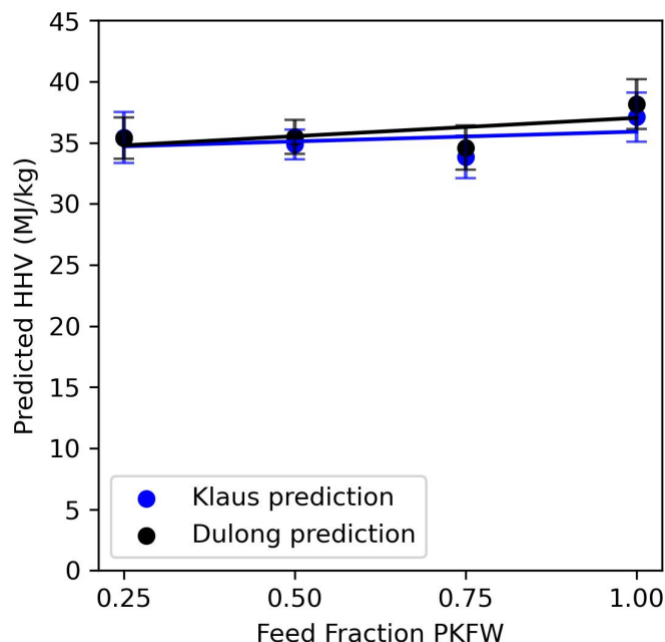


*Figure 19: Heuristic HHV for oils produced using various feed ratios. Data for oils produced with 0% PKFW feed are omitted due to high moisture content.*

The HHV of an oil product is not strongly affected by the feed ratio used to produce it due to the relatively consistent elemental compositions observed for oils in this study. While these values have not been confirmed with calorimetry, heuristic approximations of HHV have been extensively proven to be effective.

## 4.4 Carbon Balances

The total carbon balance is the most wholistic representation of the product distributions for HTL reactions available with the characterizations completed in this study. Figure 20 shows the overall carbon balance for each of the feed ratios. As in previous figures, values are determined by an average of at least two trials for each feed ratio. Error bars are defined as +/- one standard deviation.

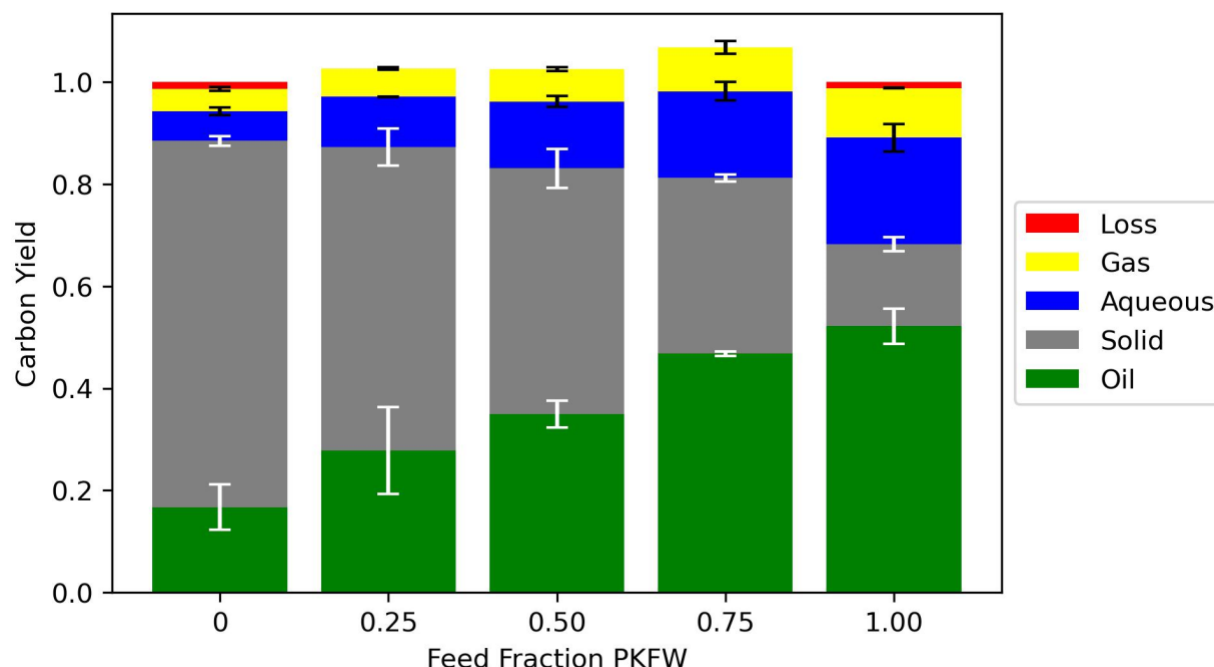


*Figure 20: Average carbon yields for each product phase of HTL reactions with various feed ratios of PKFW and lignin.*

As discussed in chapter 3, the carbon yield for each product phase was determined using elemental analysis, total organic content analysis, and the ideal gas law. All values are reported on a dry basis: carbon content of the solid and oil phases has been adjusted to account for moisture. The feed ratio was found to have little impact on elemental composition (and thus the predicted HHV) of the oil and solid products. The primary effect of altering the feed ratio between PKFW and lignin for mixed feed HTL is a shift in carbon yield from the solid product in high lignin feed reactions to the oil and, to a lesser extent, aqueous and gas phases in high PKFW feed reactions. Higher feed ratios of lignin to PKFW result in higher solid carbon yields, while higher feed ratios of PKFW to lignin result in higher oil, aqueous, and gas carbon yields. To better visualize these trends, Figures 21 through 24 show the carbon yield as a function of feed ratio for each product phase independently.

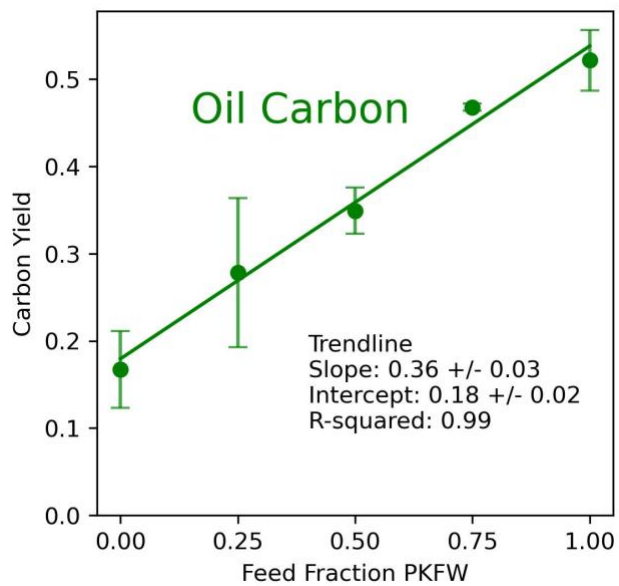


Figure 21: Carbon yield as a function of feed ratio for oil.

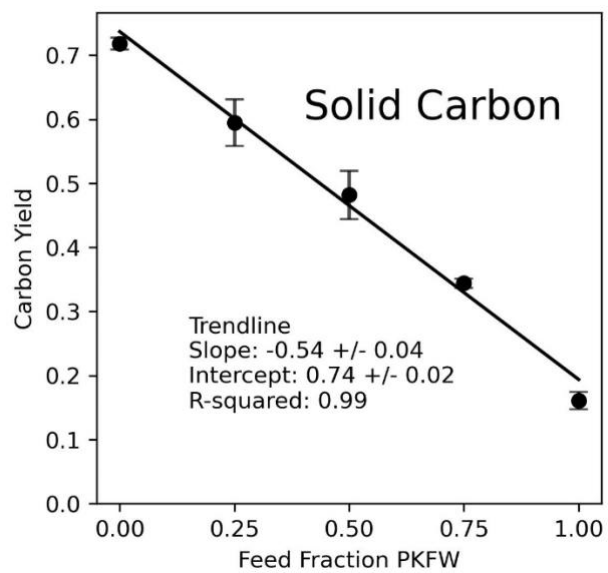


Figure 22: Carbon yield as a function of feed fraction for solid products.



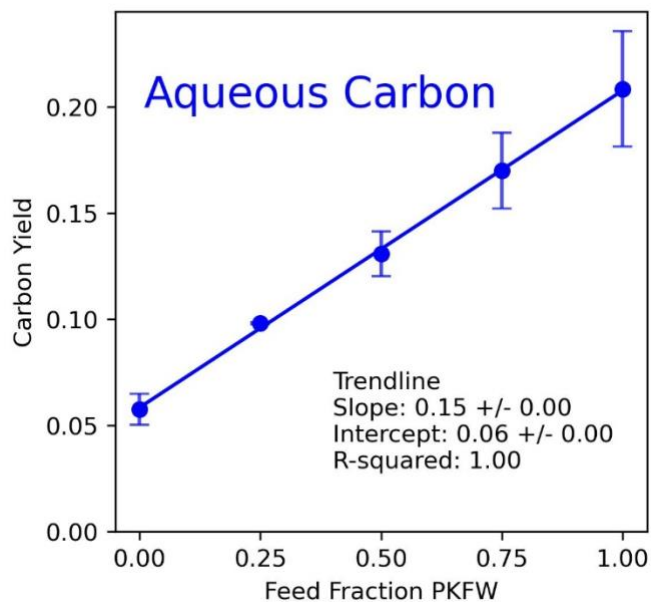


Figure 23: Carbon yield as a function of feed fraction for aqueous phase products.

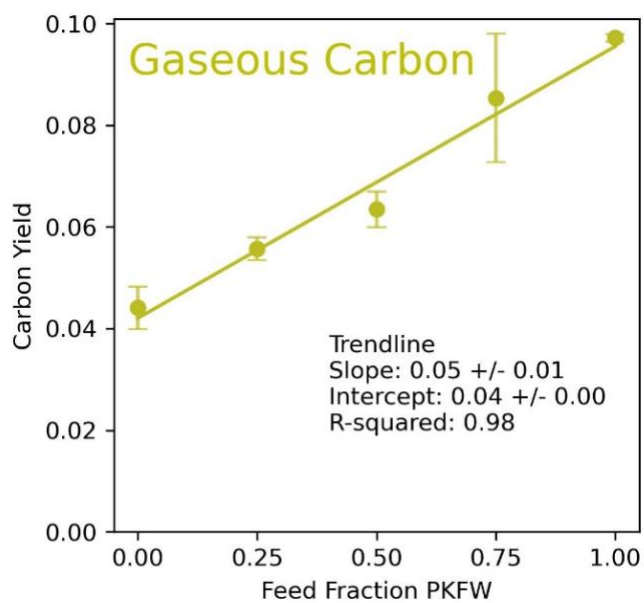
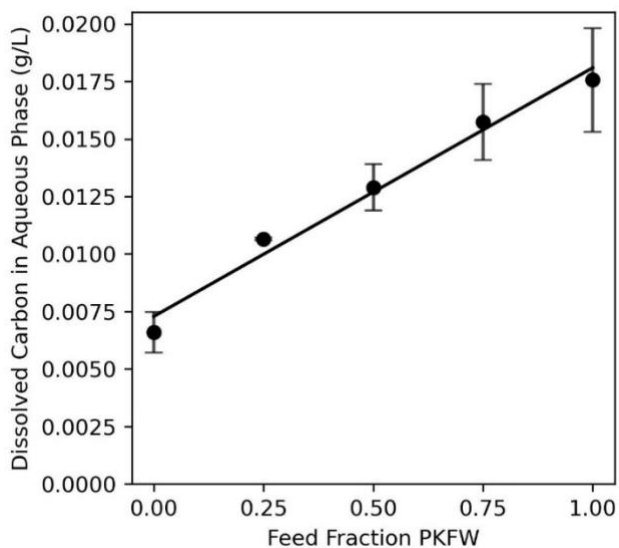


Figure 24: Carbon yield as a function of feed fraction for gas phase products.

Figure 25 shows the aqueous organic content for each feed ratio as determined by TOC, which is closely linked to the aqueous carbon yield.



*Figure 25: Dissolved carbon in aqueous phase as a function of feed fraction PKFW.*

The carbon yields for each product phase follow remarkably linear trends, with R-squared values no less than 0.97. The errors in the data and trendline uncertainties (determined by a bootstrap method with 100 iterations) are all very low, indicating a very good linear fit for the data. A table of carbon yield data may be found in Appendix C.

These results suggest a lack of significant synergistic or antagonistic effects for this system of feeds. The synergistic effect between food waste and lignocellulosic green waste observed by LeClerc et al. was largely a result of the Maillard reaction between reducing sugars and amino acids. The reducing sugars responsible for this reaction were a result of the decomposition of the cellulosic and hemicellulosic fractions of the green waste [11], which are absent from the pure lignin feed used in this study.

## 4.5 Gas Chromatography with Mass Spectrometry

Biocrude samples were analyzed by gas chromatography with mass spectrometry (GCMS) to determine trends in molecular composition. Figure 26 below shows a series of chromatograms produced by oils of each feed ratio.

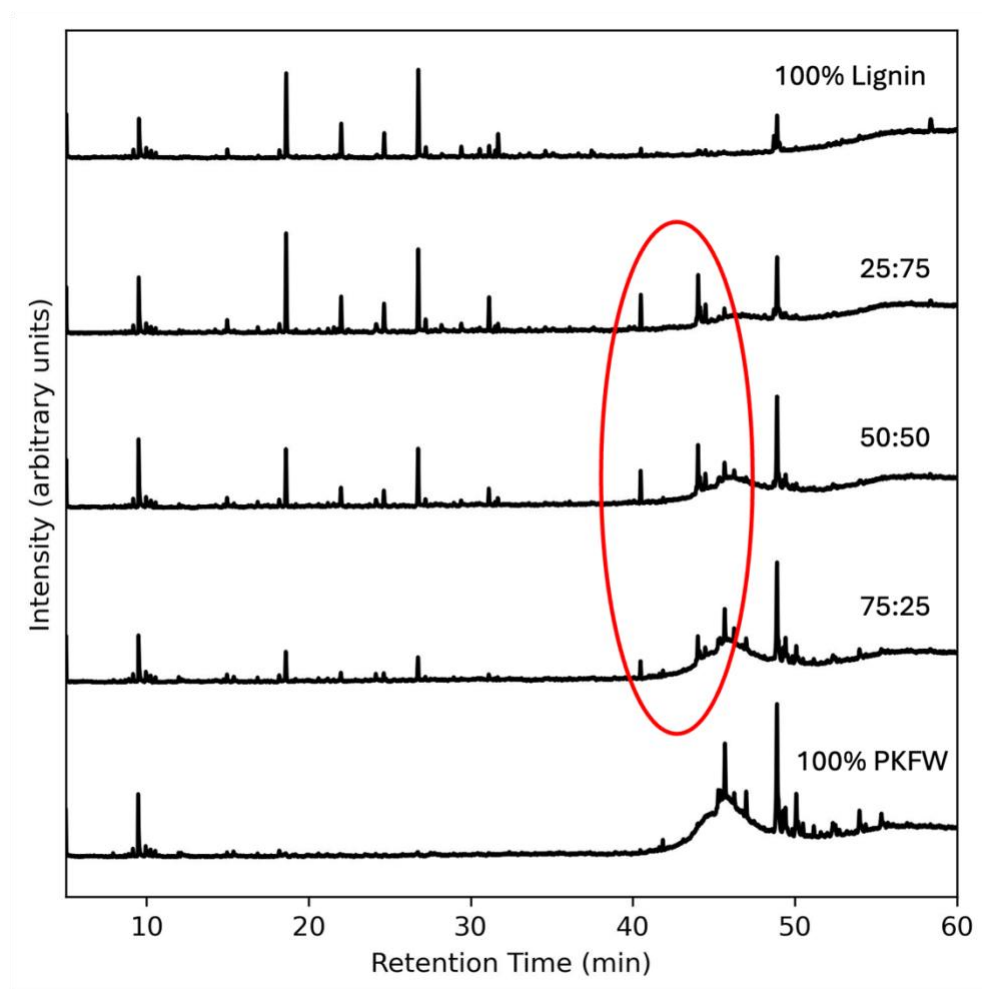


*Figure 26: GCMS chromatograms for oils produced using various feed ratios of PKFW and lignin. Emergent chemical compounds are circled for clarity.*

Since GC separates molecules on a basis of mass, this figure shows that the distribution of molecules found in mostly lignin-fed oils is generally lighter than the distribution of

molecules found in mostly PKFW-fed oils. Oils produced with only lignin feed (0% PKFW) are mostly light aromatic compounds. Very few peaks are observed at longer retention times for this oil, indicating a lack of heavy components. On the other hand, the oil produced from 100% PKFW feed comprises mostly heavy molecules, particularly long-chain fatty acids. No significant peak is observed in the chromatogram for this oil between retention times of 10 to 40 minutes.

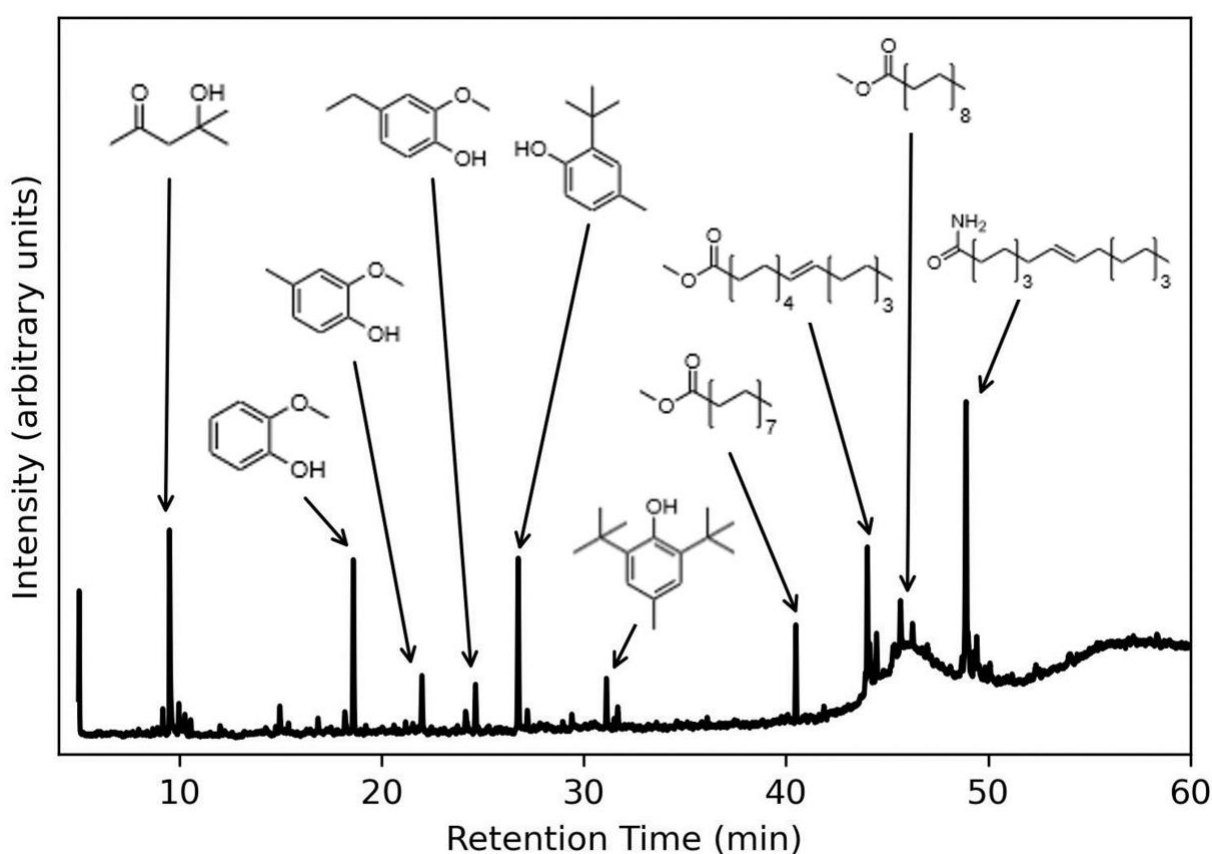


Figure 27: Significant molecular components of oil produced using a 50% PKFW feed ratio, as determined by GCMS.

Oils produced by a mixture of these two feeds contain a combination of peaks in both the low and high retention regions of the chromatogram. The magnitude of peaks associated with

each pure feed appears to be roughly proportional to the feed ratio for these mixed-feed oils. However, the method used to gather this data is not quantitative, so this observation is merely speculative. The chromatogram produced by the 50% PKFW oil was used for further molecular analysis, as shown in Figure 27.

Several of the largest peaks are labeled with the corresponding molecular structure. The low-retention peaks are mostly the products of lignin decomposition, as evidenced by their prominence in the 0% PKFW chromatogram. As would be expected, the structures of the molecules responsible for these peaks are similar to coniferyl and sinapyl alcohols, two of the major monomers that comprise lignin.

Long-chain fatty acids and methyl esters begin to appear at a retention time of about 40 minutes. The methyl esters of palmitic and oleic acid have distinct peaks at 40.49 minutes and 44.02 minutes, respectively. Palmitic and oleic acid were both identified in the broad hump of the baseline at 43 – 50 minutes. No single peaks were observed for these acids, likely due to poor acid separation caused by a degraded GC column.

Most notably, the methyl esters of palmitic and oleic acid were only observed in the mixed feed trials, suggesting chemical interaction between the lignin and food waste. Although the method used in this study was not quantitative, the 25% PKFW oil appears to have the highest concentration of these compounds. These results are consistent with LeClerc et al., who suggest that the presence of fatty acid methyl esters is the result of esterification reactions between methanol (derived from hydrolysis of methoxy phenols), and long chain fatty acids [11].

## 5.0 Conclusion

Kitchen food waste and CELF-derived lignin were studied for use in hydrothermal co-liquefaction reactions to produce sustainable biocrude. Food waste is comprised of highly energy-dense molecules such as long chain fatty acids that are known to produce high quality biocrude. The energy density and potential to offset landfill greenhouse gas emissions make food waste an appealing feed for use in HTL. On a mass basis, lignin produces significantly lower oil yields than food waste. As a byproduct of wood-pulping, however, lignin is abundant, cheap, and difficult to dispose of. Successfully utilizing lignin for energy production would be massively beneficial to both the environment and the energy industry.

Mixed feeds have the potential to enable new chemical pathways and promote higher oil yield in mixed feed HTL reactions. Combinations of feeds similar to those used in this study have enabled synergistic effects on oil yield, including food waste and lignocellulosic biomass. This result provided the motivation for this study: investigate possible synergistic effects between lignin and food waste in mixed feed HTL reactions.

Reactions were conducted in at least duplicates with pure food waste, lignin and three ratios of the two feeds, while maintaining total input feed mass and reaction conditions. An array of characterizations was performed on the reaction products to fully understand the distribution of mass and carbon. Product yields were quantified by both total mass and carbon mass, providing a comprehensive outline of the path of carbon from the feeds to the various product phases.

Feed ratio of food waste to lignin had a negligible impact on product yields outside of mixing effects. Mass yields, carbon yields, elemental compositions, and most other

characteristics of the products may be accurately predicted with a linear interpolation between the two pure feeds. The synergistic and antagonistic interactions observed for other feed combinations are mostly absent from this system. The beneficial chemistries observed between food waste and lignocellulosic biomass are largely a result of interactions between amino acids present in the food waste and cellulose present in the biomass [11]. Since lignin is a separate fraction of biomass from hemicellulose and cellulose, there is no significant source of cellulose in this system of feeds.

Gas chromatography with mass spectrometry was used to analyze the compositions of oil products for each of the feed ratios. Most of the molecular components of mixed-feed oils were found in at least one of the pure-feed oils, confirming the absence of large-scale synergistic chemistry between the feeds. However, the presence of fatty acid methyl esters in the mixed-feed oils suggests the presence of minor chemical interactions between the two feeds. LeClerc et al. suggest that fatty acid methyl esters are produced by esterification reactions between fatty acids and methanol, which arises from the decomposition of lignin. While interesting, this interaction had a negligible impact on product yields.

## 6.0 Recommendations

Food waste and lignin showed no significant synergistic or antagonistic effects as co-feeds for HTL reactions. This makes this system of feeds potentially less useful than similar feed combinations that do show significant synergistic effects in the desired range of feed ratios. However, these feeds also showed no significant antagonistic effects. Lignin is a more appealing co-feed to food waste than lignocellulosic biomass in the range of 25% food waste due to the antagonistic interaction between the cellulose and hemicellulose fractions of the biomass with the food waste [11].

The simplicity of the interaction between food waste and lignin may make the combination more appealing for large scale HTL projects. Oil yield and quality scale linearly with feed ratio, so there is no chemically-defined optimum point. Operators may select a feed ratio according to economics or feed availability rather than chemistry. For this reason, this mixture of feeds may be appealing for large scale use.



## 7.0 Future Work

While neither synergistic nor antagonistic effects were observed for this system of feeds, hydrothermal co-liquefaction of novel feed mixtures still merits further investigation. Radical initiation and catalysts have both been shown to improve biocrude yield and quality and may possibly be combined with mixed feed HTL for even better results. However, little investigation has been done in this field.

This study is an investigation of the effect of various feed ratios of PKFW and lignin on product yields for HTL. However, the results provide little information about the chemistry taking place during these reactions. Further work may investigate the molecular compositions of the feeds and products in more depth to provide a better chemical understanding of the materials used and produced in this study.

## 8.0 Acknowledgements

This project would not have been possible without the wonderful people of the waste-to-energy research group. I would like to thank my advisors, Michael Timko and Alex Maag for their constant support and unending patience through the MQP process, and for giving me the opportunity to work in the lab for the past two and a half years. I am extremely grateful for this experience which has shaped my career goals and given me invaluable hands-on training. I would also like to thank Geoffrey Tompsett, who first showed me the ropes of the lab and has always been around to lend a helping hand ever since. The basement of Goddard Hall was always a pleasant place to be thanks to Alex and Geoff. I would also like to thank David Kenny for training me on the TOC instrument and Heather LeClerc for providing the inspiration for this project and helping me figure out what I want to do after graduation.

## References

- (1) Ritchie, H.; Roser, M. *Emissions by Sector*. Our World in Data. <https://ourworldindata.org/emissions-by-sector>.
- (2) Lindsey, R. *Climate Change: Atmospheric Carbon Dioxide*. Climate.gov. <https://www.climate.gov/news-features/understanding-climate/climate-change-atmospheric-carbon-dioxide>.
- (3) Lindsey, R.; Dahlman, L. *Climate Change: Global Temperature*. Climate.gov. <https://www.climate.gov/news-features/understanding-climate/climate-change-global-temperature>.
- (4) Holladay, J.; Abdullah, Z.; Heyne, J. *Sustainable Aviation Fuel Review of Technical Pathways*; 2020. <https://www.energy.gov/sites/prod/files/2020/09/f78/beto-sust-aviation-fuel-sep-2020.pdf>.
- (5) Maag, A.; Paulsen, A.; Amundsen, T.; Yelvington, P.; Tompsett, G.; Timko, M. Catalytic Hydrothermal Liquefaction of Food Waste Using CeZrOx. *Energies* **2018**, *11* (3), 564. <https://doi.org/10.3390/en11030564>.
- (6) US EPA. *From Farm to Kitchen: The Environmental Impacts of U.S. Food Waste*. [www.epa.gov](http://www.epa.gov). <https://www.epa.gov/land-research/farm-kitchen-environmental-impacts-us-food-waste>.
- (7) Appels, L.; Lauwers, J.; Degreève, J.; Helsen, L.; Lievens, B.; Willems, K.; Van Impe, J.; Dewil, R. Anaerobic Digestion in Global Bio-Energy Production: Potential and Research Challenges. *Renewable and Sustainable Energy Reviews* **2011**, *15* (9), 4295–4301. <https://doi.org/10.1016/j.rser.2011.07.121>.
- (8) Kirubakaran, V.; Sivaramakrishnan, V.; Nalini, R.; Sekar, T.; Premalatha, M.; Subramanian, P. A Review on Gasification of Biomass. *Renewable and Sustainable Energy Reviews* **2009**, *13* (1), 179–186. <https://doi.org/10.1016/j.rser.2007.07.001>.
- (9) Demirbas, A.; Arin, G. An Overview of Biomass Pyrolysis. *Energy Sources* **2002**, *24* (5), 471–482. <https://doi.org/10.1080/00908310252889979>.
- (10) Gollakota, A. R. K.; Kishore, N.; Gu, S. A Review on Hydrothermal Liquefaction of Biomass. *Renewable and Sustainable Energy Reviews* **2018**, *81*, 1378–1392. <https://doi.org/10.1016/j.rser.2017.05.178>.

(11) LeClerc, H. O.; Page, J. R.; Tompsett, G. A.; Niles, S. F.; McKenna, A. M.; Valla, J. A.; Timko, M. T.; Teixeira, A. R. Emergent Chemical Behavior in Mixed Food and Lignocellulosic Green Waste Hydrothermal Liquefaction. *ACS Sustainable Chemistry & Engineering* **2022**, *11* (6), 2427–2439. <https://doi.org/10.1021/acssuschemeng.2c06266>.

(12) Yang, J.; Sophia He, Q.; Yang, L. A Review on Hydrothermal Co-Liquefaction of Biomass. *Applied Energy* **2019**, *250*, 926–945. <https://doi.org/10.1016/j.apenergy.2019.05.033>.

(13) Yang, L.; He, Q.; Havard, P.; Corscadden, K.; Chunbao (Charles) Xu; Wang, X. Co-Liquefaction of Spent Coffee Grounds and Lignocellulosic Feedstocks. *Bioresource Technology* **2017**, *237*, 108–121. <https://doi.org/10.1016/j.biortech.2017.02.087>.

(14) *Athens – Athens Services*. [Athensservices.com](https://athensservices.com/). <https://athensservices.com/>.

(15) Motofumi Saisu; Sato, T.; Watanabe, M.; Tadafumi Adschiri; Arai, K. Conversion of Lignin with Supercritical Water–Phenol Mixtures. *Energy & Fuels* **2003**, *17* (4), 922–928. <https://doi.org/10.1021/ef0202844>.

(16) Yoo, C. G.; Dumitrache, A.; Muchero, W.; Natzke, J.; Akinosho, H.; Li, M.; Sykes, R. W.; Brown, S. D.; Davison, B.; Tuskan, G. A.; Pu, Y.; Ragauskas, A. J. Significance of Lignin S/G Ratio in Biomass Recalcitrance of *Populus Trichocarpa* Variants for Bioethanol Production. *ACS Sustainable Chemistry & Engineering* **2017**, *6* (2), 2162–2168. <https://doi.org/10.1021/acssuschemeng.7b03586>.

(17) Bajwa, D. S.; Pourhashem, G.; Ullah, A. H.; Bajwa, S. G. A Concise Review of Current Lignin Production, Applications, Products and Their Environmental Impact. *Industrial Crops and Products* **2019**, *139*, 111526. <https://doi.org/10.1016/j.indcrop.2019.111526>.

(18) Meng, X.; Parikh, A.; Seemala, B.; Kumar, R.; Pu, Y.; Christopher, P.; Wyman, C. E.; Cai, C. M.; Ragauskas, A. J. Chemical Transformations of Poplar Lignin during Cosolvent Enhanced Lignocellulosic Fractionation Process. *ACS Sustainable Chemistry & Engineering* **2018**, *6* (7), 8711–8718. <https://doi.org/10.1021/acssuschemeng.8b01028>.

(19) Eero Sjoestroem. *Wood Chemistry : Fundamentals and Applications.*; New York (U.S.A.) Academic Press (Erschienen), 1981.

(20) *Carbon Testing | Elemental Testing and Analysis | Midwest Microlab*. Analysis of Carbon, Hydrogen, Nitrogen, Oxygen, and halogens including Fluorine. <https://midwestlab.com/elemental-analysis-services/carbon-testing/>.

(21) Kathiravale, S.; Noor Muhd Yunus, M.; Sopian, K.; Samsuddin, A. H.; Rahman, R. A. Modeling the Heating Value of Municipal Solid Waste\*. *Fuel* **2003**, 82 (9), 1119–1125. [https://doi.org/10.1016/s0016-2361\(03\)00009-7](https://doi.org/10.1016/s0016-2361(03)00009-7).

(22) Schmidt-Rohr, K. Why Combustions Are Always Exothermic, Yielding about 418 KJ per Mole of O<sub>2</sub>. *Journal of Chemical Education* **2015**, 92 (12), 2094–2099. <https://doi.org/10.1021/acs.jchemed.5b00333>.

(23) *TOC-L Series*. [www.ssi.shimadzu.com](http://www.ssi.shimadzu.com). <https://www.ssi.shimadzu.com/products/total-organic-carbon-analysis/toc-analysis/toc-l-series/index.html> (accessed 2023-06-23).

(24) Bisutti, I.; Hilke, I.; Raessler, M. Determination of Total Organic Carbon – an Overview of Current Methods. *TrAC Trends in Analytical Chemistry* **2004**, 23 (10-11), 716–726. <https://doi.org/10.1016/j.trac.2004.09.003>.

(25) Cheng, F.; Tompsett, G. A.; Murphy, C. M.; Maag, A. R.; Carabillo, N.; Bailey, M.; Hemingway, J. J.; Romo, C. I.; Paulsen, A. D.; Yelvington, P. E.; Timko, M. T. Synergistic Effects of Inexpensive Mixed Metal Oxides for Catalytic Hydrothermal Liquefaction of Food Wastes. *ACS Sustainable Chemistry & Engineering* **2020**, 8 (17), 6877–6886. <https://doi.org/10.1021/acssuschemeng.0c02059>.

(26) *Titration EasyPlus Easy KFV*. [www.mt.com](http://www.mt.com). [https://www.mt.com/us/en/home/products/Laboratory\\_Analytics\\_Browse/Product\\_Family\\_Browse\\_titrators\\_main/easyplus-titration/easyplus-automated-titrators/easyplus-titrator-easy-kfv.html](https://www.mt.com/us/en/home/products/Laboratory_Analytics_Browse/Product_Family_Browse_titrators_main/easyplus-titration/easyplus-automated-titrators/easyplus-titrator-easy-kfv.html) (accessed 2023-06-23).

(27) Connors, K. A. The Karl Fischer Titration of Water. *Drug Development and Industrial Pharmacy* **1988**, 14 (14), 1891–1903. <https://doi.org/10.3109/03639048809151996>.

(28) Santos, F. J.; Galceran, M. T. Modern Developments in Gas Chromatography-Mass Spectrometry-Based Environmental Analysis. *Journal of Chromatography* **2003**, 1000 (1-2), 125–151. [https://doi.org/10.1016/s0021-9673\(03\)00305-4](https://doi.org/10.1016/s0021-9673(03)00305-4).

## Appendix

### Appendix A: Selected images of feed and reactor setup



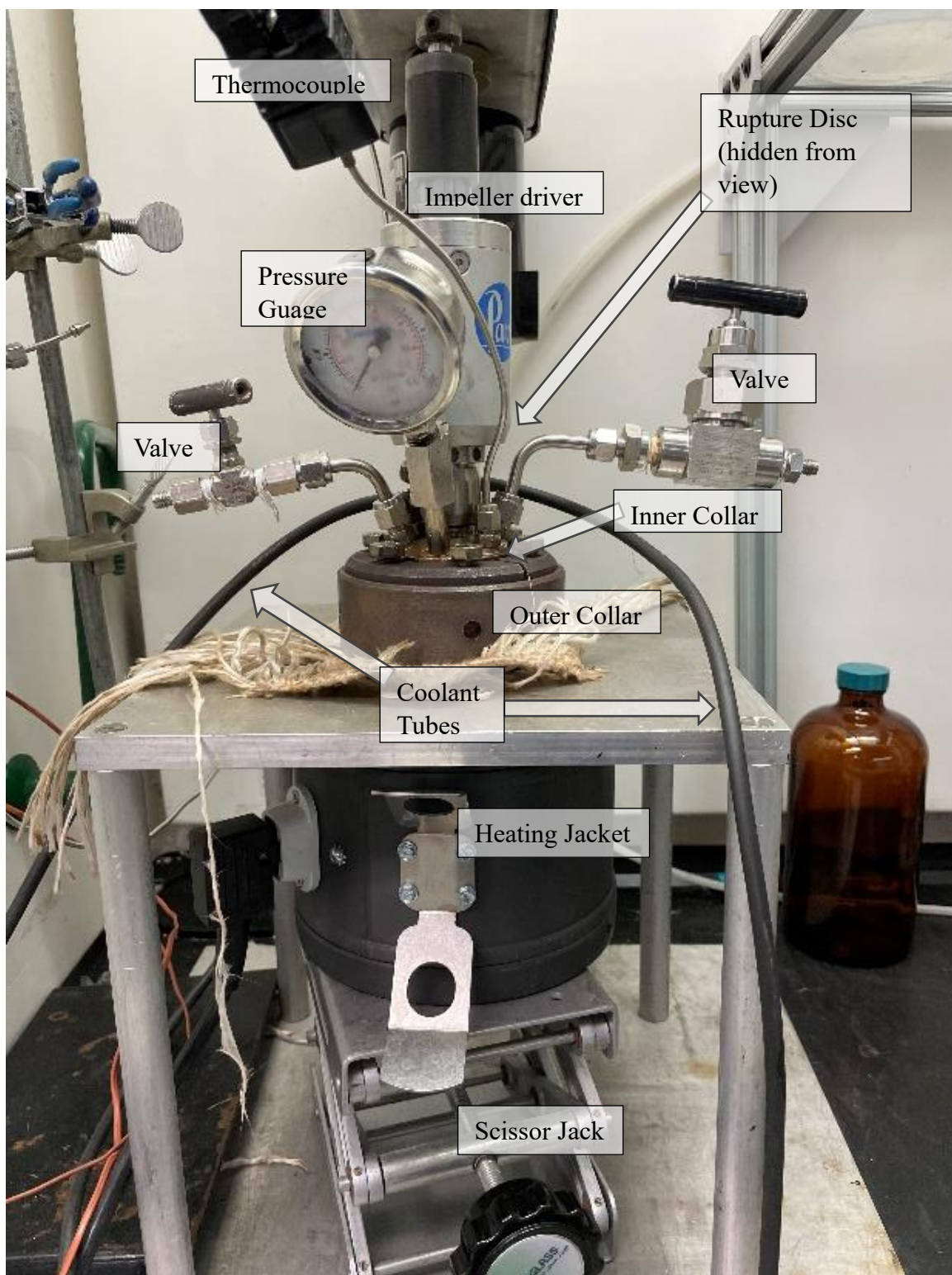
Dry CELF-derived lignin used as a feed in this study. The lignin was produced by researchers at University of California Riverside from green waste sourced from Athens Services of City of Industry, California. The lignin has been stored in a freezer since arriving at WPI.



Frozen wet prison kitchen food waste (PKFW) used in this study. The waste was produced at Coyote Ridge Correctional Facility, autoclaved on 3/20/2021, and shipped to WPI where it has been stored in a freezer.



Top-down view of reactor bottom after addition of feeds and water.



HTL reactor prior to nitrogen purge and pressurization. Important components are labeled.





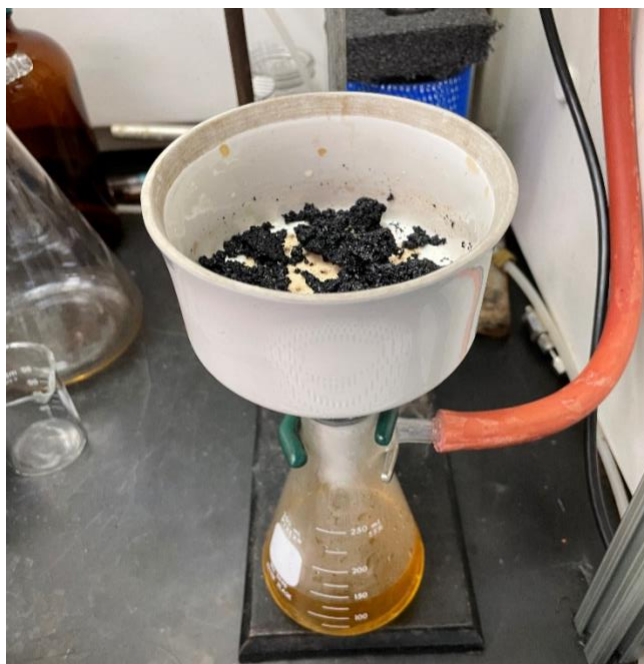
HTL reactor during ice bath cooling.



Benchtop removal of reactor collar. The inner collar is visible, securing the head and bottom of the reactor together. The collar is fastened with six bolts.



Top-down view of reactor bottom after depressurization and reactor head removal. Clumps of solid phase product are visible floating in the aqueous phase.



Vacuum filtration for separation of the aqueous phase from the solid and oil phases.



Rotary evaporation of oil/acetone mixture.



Isolated oil phase product in a 1-dram vial.



Isolated aqueous phase after vacuum filtration, stored in three individual 5-dram vials. All vials pictured were sourced from the same reaction.

## Appendix B: Sample instrument reports and tracking sheets

Date: 02/15/2023

Run Name: HTL-PKFW-Lignin-50:50-3

Operator(s): SBK

**Reactant Identities:**

Feed (name): PKFW (wet), Lignin	Catalyst (name): None
------------------------------------	--------------------------

**Input Mass (g):**

(48.28) Organic Feed: PKFW 48.28	Water: (90.47) 90.50	(11.257) Catalyst: Lignin 11.26
-------------------------------------	-------------------------	------------------------------------

**Pre-Run Measurements (g):**

Reactor Top: 3233.7	Reactor Bottom: 1665.5	Whole Reactor: 5048.7
------------------------	---------------------------	--------------------------

**Reaction:**

	Initial	Start	End	Quenched
Time (XX:XX)	3:05	3:45	4:45	4:55
Temp (C)	11	300	295	40
Pressure (psi)	200	1320	1570	380

**Post-Run Measurements (g):**

Whole Reactor: 5046.5	Filter Paper, Funnel, Stopper: 293.77	Filter Paper, Funnel, Stopper, Oil, Char: 309.67	Filter Paper, Funnel, Stopper, Char: 303.55
Empty Aqueous Flask: 170.53	Full Aqueous Flask: 204.55	Empty Round-Bottom Flask: 381.84	Full Round-Bottom Flask: 387.65
Reactor Top: 3234.2	Reactor Bottom: 1665.8	Empty Vial, Label: 51.56	Char, Vial, Label (undried): 59.59
		Char, Vial, Label (dried): 57.79	

**Notes:**

New seal

Sample tracking sheet used for HTL reactions. The sheet pictured was used for the third 50:50 PKFW:lignin feed HTL reaction



Lignin 2 oil, 1/27  
SAMPLE IDENTIFICATION ON Vial

Analysis Requested: Elemental Analysis

Single  Duplicate  Triplicate

Submitter Name:	[REDACTED]
Business or Institution:	[REDACTED]
Lab Group:	[REDACTED]
Results email and Phone #:	[REDACTED]
Invoice email and Phone#:	[REDACTED]
Invoice Address:	[REDACTED]
Purchase Order Number:	[REDACTED]

Analysis Requested	Customer Theory	Office Use Only: Results are total % Found		
C	70	64.72		
H	5	7.01		
N	5	0.52		

Molecular Formula:	C <sub>6</sub> H <sub>5</sub> N <sub>0.4</sub> O <sub>1.3</sub>
Air Sensitive/ Glove Box:	YES <input type="checkbox"/> NO <input checked="" type="checkbox"/>
Hazardous/ Explosive:	YES <input type="checkbox"/> NO <input checked="" type="checkbox"/>
Hydroscopic:	YES <input type="checkbox"/> NO <input checked="" type="checkbox"/>
Vacuum Drying Requested:	Temp: _____ °C Time: ___ Hr. ___ Min.
Yes	<input type="checkbox"/>
No	<input checked="" type="checkbox"/>
Sample Return Address:	
Yes	<input type="checkbox"/>
No	<input checked="" type="checkbox"/>

Shipping address:  
Midwest Microlab  
Attn: Valerie Guzzetta  
7212 N. Shadeland Ave., Suite 110  
Indianapolis, IN 46250  
Phone: 317-849-6606  
Fax: 317-849-8534  
Email: info@midwestlab.com  
Website: www.midwestlab.com

Submitter Comments:

**sample is char solid containing carbon, hydrogen, oxygen and nitrogen with trace sulfur and ash**

-----  
*Office Use Only*

Please include 1 submission form per sample.

We appreciate your business.

RECEIVED FEB 07 2023

Example elemental analysis report issued by Midwest Microlabs. The report pictured is for the oil product of the second HTL run using pure lignin feed.

Solvent (MeOH)	✓	N/A		4.09685	3.6205	0.4760	0.01	0.01
				3.6205	3.1085	0.5120	0.01	
				3.1085	2.6217	0.4868	0.02	43.3% NSD
HTL Lignin-1	0.2058	2.0243	0.0923	4.0322	3.5701	0.4621	0.39	6.35
				3.5701	3.1070	0.4631	0.36	0.8
				3.1070	2.6341	0.4729	0.29	NSD
HTL-RFW-2	0.2164	2.0897	0.0938	3.9598	3.4694	0.4904	0.12	0.12
				3.4694	3.0935	0.3759	0.12	
				3.0935	2.6345	0.4582	0.12	0.0% NSD
HTL Lignin-2	0.2669	2.0723	0.1141	3.9432	3.5106	0.4326	7.18	7.14
			1x	3.5106	3.0926	0.4180	7.21	1.4%
				3.0926	2.6364	0.4562	7.03	NSD
	2.2301	2.3061	2.3392					

Sample tracking sheet used for Karl Fisher titration analysis

# TOC-Control L Report

DK  
SBK\_PKFW\_Lignin\_02\_03\_2023.tlx

## Instr. Information

Instrument Options  
Catalyst

TOC/ASI/IC Unit/  
High Sensitivity

## Cal. Curve

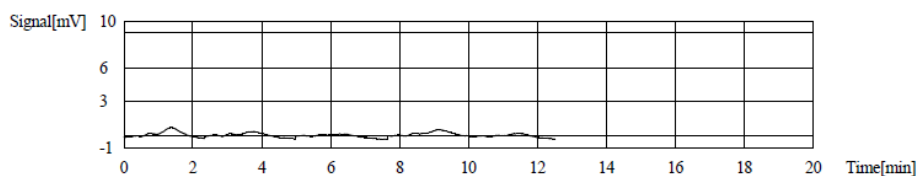
Sample Name: Standards  
Sample ID: Standards  
Cal. Curve: DK NPOC 10ppm.2023\_02\_03\_15\_18\_07.cal  
Status: Completed

Type	Anal.
Standard	NPOC

Conc: 0.000mg/L

No.	Area	Inj. Vol.	Aut. Dil.	Rem.	Ex.	Date / Time
1	3.941	50uL	1.000	*****		2/3/2023 3:26:26 PM
2	3.218	50uL	1.000	*****		2/3/2023 3:29:19 PM
3	1.928	50uL	1.000	*****	E	2/3/2023 3:32:19 PM
4	3.056	50uL	1.000	*****		2/3/2023 3:34:58 PM
5	2.279	50uL	1.000	*****	E	2/3/2023 3:37:41 PM

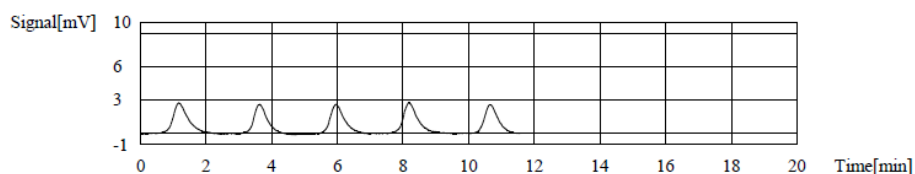
Acid Add. 0.000%  
Spurge Gas Flow 80mL/min  
Sp. Time 90.00sec  
Mean Area 3.405



Conc: 2.000mg/L

No.	Area	Inj. Vol.	Aut. Dil.	Rem.	Ex.	Date / Time
1	9.218	50uL	1.000	*****	E	2/3/2023 3:46:45 PM
2	7.974	50uL	1.000	*****		2/3/2023 3:49:21 PM
3	8.352	50uL	1.000	*****		2/3/2023 3:51:49 PM
4	8.504	50uL	1.000	*****		2/3/2023 3:54:41 PM
5	7.600	50uL	1.000	*****	E	2/3/2023 3:57:00 PM

Acid Add. 0.000%  
Spurge Gas Flow 80mL/min  
Sp. Time 90.00sec  
Mean Area 8.277

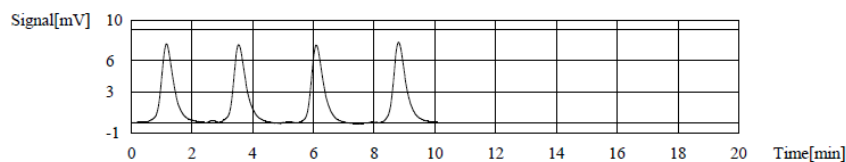


Conc: 6.000mg/L

No.	Area	Inj. Vol.	Aut. Dil.	Rem.	Ex.	Date / Time
1	22.15	50uL	1.000	*****		2/3/2023 4:06:08 PM
2	23.01	50uL	1.000	*****	E	2/3/2023 4:08:56 PM
3	22.22	50uL	1.000	*****		2/3/2023 4:11:56 PM
4	22.69	50uL	1.000	*****		2/3/2023 4:14:37 PM



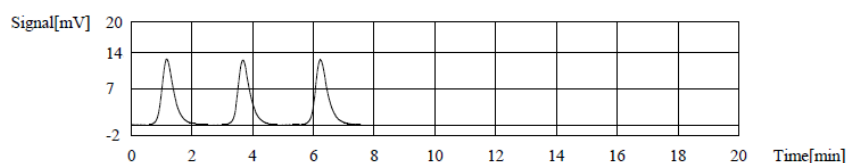
Acid Add. 0.000%  
 Spurge Gas Flow 80mL/min  
 Sp. Time 90.00sec  
 Mean Area 22.35



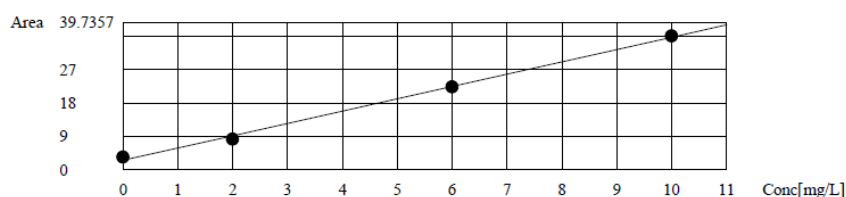
Conc: 10.00mg/L

No.	Area	Inj. Vol.	Aut. Dil.	Rem.	Ex.	Date / Time
1	35.86	50ul	1.000	*****		2/3/2023 4:23:44 PM
2	35.98	50ul	1.000	*****		2/3/2023 4:26:32 PM
3	36.53	50ul	1.000	*****		2/3/2023 4:29:27 PM

Acid Add. 0.000%  
 Spurge Gas Flow 80mL/min  
 Sp. Time 90.00sec  
 Mean Area 36.12



Slope: 3.325  
 Intercept 2.576  
 r<sup>2</sup> 0.9974  
 r 0.9987  
 RSE(%) N/A  
 Zero Shift No



Example TOC calibration report using a diluted KHP standard. This calibration was performed before every batch of samples analyzed using the instrument

#### Sample

Sample Name: HTL\_Lignin\_1  
 Sample ID: L1  
 Origin: DK NPOC 10ppm.met  
 Status: Completed  
 Chk. Result

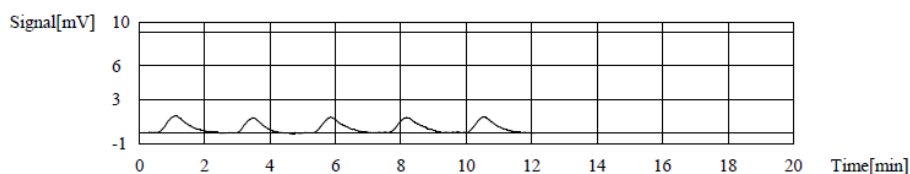
Type	Anal.	Manual Dilution	Result
Unknown	NPOC	1.000	NPOC:1.082mg/L

1. Det

Anal.: NPOC

No.	Area	Conc.	Inj. Vol.	Aut. Dil.	Ex.	Cal. Curve	Date / Time
1	6.200	1.090mg/L	50ul	1.000		DK NPOC 10ppm.2023_02_03_15_18_07.cal	2/3/2023 4:58:28 PM
2	5.313	0.8232mg/L	50ul	1.000	E	DK NPOC 10ppm.2023_02_03_15_18_07.cal	2/3/2023 5:01:05 PM
3	5.939	1.011mg/L	50ul	1.000	E	DK NPOC 10ppm.2023_02_03_15_18_07.cal	2/3/2023 5:03:39 PM
4	6.159	1.078mg/L	50ul	1.000		DK NPOC 10ppm.2023_02_03_15_18_07.cal	2/3/2023 5:06:17 PM
5	6.162	1.079mg/L	50ul	1.000		DK NPOC 10ppm.2023_02_03_15_18_07.cal	2/3/2023 5:09:13 PM

Mean Area 6.174  
 Mean Conc. 1.082mg/L  
 SD Area 0.02285  
 CV Area 0.37%



Example TOC report for analysis of a single sample. The analysis report pictured is for the aqueous phase produced by the second HTL reaction using a pure lignin feed.

## Appendix C: Tables of Data

*Table 2: Average mass yields of each product phase for each feed ratio. Error was determined by standard deviation. The mass yield of oil relative to the feedstock was determined by dividing oil yield mass by the dry mass of feed used for the reaction.*

	0% PKFW	25% PKFW	50% PKFW	75% PKFW	100% PKFW
Oil	0.98% ± 0.13%	2.97% ± 0.64%	3.93% ± 0.32%	5.14% ± 0.17%	5.18% ± 0.12%
Oil (relative to feed)	6.52% ± 0.86%	19.82% ± 4.27%	26.33% ± 2.12%	34.51% ± 1.04%	34.53% ± 0.84%
Solid	9.08% ± 0.05%	7.24% ± 0.68%	5.27% ± 0.30%	3.56% ± 0.07%	1.68% ± 0.09%
Aqueous	81.77% ± 0.77%	81.57% ± 0.05%	84.52% ± 0.32%	84.64% ± 0.32%	87.85% ± 0.21%
Gas	1.51% ± 0.14%	1.81% ± 0.07%	1.94% ± 0.11%	2.45% ± 0.35%	2.64% ± 0.02%
Loss	6.66% ± 0.71%	6.41% ± 0.09%	4.35% ± 1.05%	4.21% ± 0.21%	2.66% ± 0.02%

*Table 3: Average elemental compositions for oils produced by reactions using each feed ratio. Values are reported on a dry basis. Oils produced using 0% PKFW are omitted due to high moisture.*

	25% PKFW	50% PKFW	75% PKFW	100% PKFW
Carbon	81.92% ± 7.75%	74.02% ± 0.28%	71.31% ± 2.71%	74.45% ± 3.13%
Hydrogen	6.57% ± 1.17%	8.81% ± 0.75%	9.00% ± 0.31%	10.17% ± 0.34%
Nitrogen	2.47% ± 0.40%	2.84% ± 0.22%	4.01% ± 0.37%	5.78% ± 0.13%
Oxygen	10.38% ± 6.62%	15.21% ± 1.24%	17.54% ± 3.26%	12.25% ± 3.69%

*Table 4: Average elemental compositions for solids produced by reactions using each feed ratio. Values are reported on a dry basis.*

	0% PKFW	25% PKFW	50% PKFW	75% PKFW	100% PKFW
Carbon	73.93% ± 0.34%	72.71% ± 2.40%	76.03% ± 1.74%	75.66% ± 0.43%	70.87% ± 2.20%
Hydrogen	5.17% ± 0.01%	5.17% ± 0.09%	5.45% ± 0.33%	6.17% ± 0.41%	6.07% ± 0.36%
Nitrogen	0.97% ± 0.01%	1.79% ± 0.03%	2.70% ± 0.20%	3.84% ± 0.35%	5.71% ± 0.13%
Oxygen	19.94% ± 0.35%	20.34% ± 2.52%	15.83% ± 1.61%	14.34% ± 0.49%	17.36% ± 2.69%

Table 5: Average carbon yields of each product phase for reactions using each feed ratio.

	0% PKFW		25% PKFW		50% PKFW		75% PKFW		100% PKFW	
Oil	16.72%	± 4.40%	27.83%	± 8.55%	34.93%	± 2.68%	46.79%	± 0.39%	52.17%	± 3.46%
Solid	71.79%	± 0.94%	59.46%	± 3.64%	48.18%	± 3.79%	34.42%	± 0.72%	16.09%	± 1.32%
Aqueous	5.76%	± 0.73%	9.82%	± 0.05%	13.10%	± 1.06%	17.01%	± 1.78%	20.86%	± 2.71%
Gas	4.41%	± 0.42%	5.57%	± 0.22%	6.35%	± 0.35%	8.54%	± 1.26%	9.72%	± 0.08%
Loss	1.33%	± 2.31%	-2.68%	± 5.07%	-2.55%	± 7.88%	-6.75%	± 2.72%	1.17%	± 1.99%